

FILE COPY  
NO. 2-W

N 62 53109

# CASE FILE COPY

## NATIONAL ADVISORY COMMITTEE FOR AERONAUTICS

TECHNICAL NOTE

No. 1109

FLIGHT INVESTIGATION OF THE COOLING CHARACTERISTICS

OF A TWO-ROW RADIAL ENGINE INSTALLATION

II - COOLING-AIR PRESSURE RECOVERY AND PRESSURE DISTRIBUTION

By E. John Hill, Calvin C. Blackman, and James E. Morgan

Aircraft Engine Research Laboratory  
Cleveland, Ohio

**FILE COPY**

To be returned to  
the files of the National  
Advisory Committee  
for Aeronautics  
Washington, D. C.



Washington  
July 1946





NATIONAL ADVISORY COMMITTEE FOR AERONAUTICS

TECHNICAL NOTE NO. 1109

FLIGHT INVESTIGATION OF THE COOLING CHARACTERISTICS  
OF A TWO-ROW RADIAL ENGINE INSTALLATION

II - COOLING-AIR PRESSURE RECOVERY AND PRESSURE DISTRIBUTION

By E. John Hill, Calvin C. Blackman, and James E. Morgan

SUMMARY

Flight tests have been conducted at altitudes of 5000 and 20,000 feet to investigate the cooling-air pressure recovery and distribution for a two-row radial engine enclosed in a low-inlet-velocity cowling of a twin-engined airplane. The effect of flight variables on average recovery and circumferential, radial, and longitudinal distribution are presented for level flight; also included is a comparison of pressure-drop measurements across the engine, as indicated by nine different combinations of pressure tubes.

The results of these tests showed that pressure recovery and distribution can be greatly affected by changes in flight variables. Those variables having the greatest effect were cowl-flap angle, angle of attack of the thrust axis, and the propeller thrust disk-loading coefficient. The tests further showed that large differences, sometimes amounting to 100 percent, were obtained in the results indicated by various methods of measuring pressure drop across the engine.

On the basis of the results, it is observed that an important consideration in the design of cowlings and cowl flaps should be the obtaining of good distribution of cooling air, as well as minimum drag for the installation. The fact that these tests showed that the front recovery decreased with an increase in propeller thrust disk-loading coefficient provides additional evidence that the recovery is greatly affected by the combined propeller-nacelle design. Also of significance is that a large increase in front recovery in these tests resulted in a similar increase in rear pressure, indicating that an increase in the front recovery of an air-cooled engine is not always an effective method of increasing the cooling-air flow.





INTRODUCTION

A flight investigation of a two-row radial engine enclosed in a low-inlet-velocity cowling was undertaken to determine the cooling characteristics of the installation at altitude. The introductory report of this investigation (reference 1) was concerned with the correlation of the engine cooling variables at altitude by the method described in reference 2 and the adaptability of this correlation for the determination of the general cooling performance of the engine installation.

The present report is a study of the cooling-air pressure recovery and distribution within the engine cowling. The distribution of cooling-air flow is one of the important factors that control the distribution of temperature among the cylinders of an air-cooled multicylinder engine. Inasmuch as efficient engine operation postulates a relatively uniform temperature distribution in order to minimize cooling drag and to develop maximum power and fuel economy, a study of the factors controlling cooling-air distribution is of considerable importance.

The quantity of cooling air flowing over the individual cylinders of an air-cooled engine is mainly a function of the pressure drop across the cylinder. This pressure drop is determined by the pressure recovery and distribution at the front and the rear of the engine, which in turn are dependent upon the cowling design, flight conditions, and engine conductivity (a nondimensional factor indicative of the resistance to cooling-air flow through the engine). A large number of wind-tunnel and flight investigations have been made involving cooling-air pressure recovery and average pressure drop but they have been associated mainly with the problems of optimum cowling design. Little work has been reported concerning the effect of flight variables on the distribution of cooling-air flow.

An investigation was made at the NACA Cleveland laboratory of the cooling-air pressure recovery and distribution throughout an air-cooled engine installation and of the effect of important flight variables on recovery and distribution during level unaccelerated flight. The results are, in detail, applicable only to this engine installation; however, in the discussion an attempt is made towards a general interpretation of the results. A study of average cooling-air pressure recoveries and circumferential, radial, and longitudinal pressure distribution is included. The variables investigated were: (a) airplane speed, which influences the pressure available for cooling the engine; (b) cowl-flap angle, which changes the resistance to air flow through the cowling and also effects the cowl-exit pressure; (c) angle of attack of the thrust axis, which influences the characteristics of air flow into the cowling; (d) propeller thrust



disk-loading coefficient, which is a measure of the pressure rise across the propeller; and (e) propeller speed, which affects the rotation imparted to the air. A comparison of different pressure-drop measurements across the engine is also included.

### SYMBOLS AND COEFFICIENTS

The following symbols are used in the analysis of the investigation:

$C_s$	speed-power coefficient, $\sqrt[5]{\rho V^5 / P N^2}$
$D$	diameter of propeller
$H$	total pressure above atmospheric static pressure
$N$	propeller rotational speed
$P$	power absorbed by propeller
$p$	static pressure above atmospheric static pressure
$\Delta p$	pressure drop across engine
$q_c$	free-stream impact pressure
$S$	propeller-disk area, $\frac{\pi D^2}{4}$
$T$	thrust, $P \eta / V$
$T_c$	thrust disk-loading coefficient, $T / q_c S$
$V$	velocity relative to air stream
$V/ND$	propeller advance-diameter ratio
$\alpha$	angle of attack of thrust axis
$\beta$	blade angle of propeller at 0.75 radius
$\eta$	propeller efficiency
$\rho$	mass density of free stream





Subscripts

ae	average engine
b	barrel
e	exhaust side of cylinder
fr	front row
h	head
i	intake side of cylinder
rr	rear row
t	top of cylinder
1 to 8	logitudinal stations relative to cylinder

APPARATUS AND METHODS

Airplane and engine. - The investigation of cooling-air pressure recovery and distribution was conducted on the right engine installation of a twin-engined airplane (fig. 1). A sketch of the cowling with charge-air and oil-cooler ducts is shown in figure 2. The cowling is of the short-nose type without entrance diffuser and with cowl flaps located on both sides of the lower portion of the nacelle. Very little exit area is provided for the cooling-air flow from the cowling except through the cowl flaps, which remain partly open even in the "full-closed" position. The test engine was of the 18-cylinder, double-row radial, air-cooled type having a gear-driven, single-stage, two-speed supercharger. The conventional propeller reduction gear, which had a ratio of 2:1, was replaced with a torquemeter having the same ratio.

The propeller was four-bladed,  $13\frac{1}{2}$  feet in diameter, and of the constant-speed type; it was fitted with cuffs and spinner that are standard for this installation.

Approximate normal flight conditions for the airplane at a gross weight of 30,000 pounds are given in the following table for level flight at altitudes of 5000 and 20,000 feet for take-off and for climb:

Year	Value
1950	100
1951	105
1952	110
1953	115
1954	120
1955	125
1956	130
1957	135
1958	140
1959	145
1960	150

The following table shows the results of the survey conducted in 1960. The data indicates a steady increase in the number of respondents over the period from 1950 to 1960. The average age of the respondents was found to be 35 years, with a range from 18 to 65. The majority of respondents were male, accounting for approximately 75% of the total sample. The survey also revealed that the majority of respondents were employed, with a significant portion working in the manufacturing sector. The results suggest a positive correlation between the variables studied, indicating that the factors investigated have a significant impact on the outcomes measured. Further analysis of the data is required to determine the specific causes and effects of these trends.

The survey was conducted using a stratified random sampling method to ensure that the sample was representative of the population. The data was analyzed using statistical methods, including descriptive statistics and regression analysis. The findings of the survey are presented in the following table, which shows the distribution of responses across various categories. The results indicate that the majority of respondents are satisfied with the current state of affairs, although there is still a need for improvement in certain areas. The survey provides valuable insights into the attitudes and behaviors of the population, which can be used to inform policy-making and program development. The data also highlights the importance of continued research and monitoring to track changes over time and assess the effectiveness of interventions.



Operating condition	Altitude (ft)	Brake horse-power per engine	Engine speed (rpm)	Indicated airspeed (mph)	Angle of attack of thrust axis (deg)	Cowl-flap position
Low-power cruise	5,000	800	1800	195	4	Closed
	20,000	800	1900	170	6	Closed
Normal cruise	5,000	1050	2100	220	3	Closed
	20,000	1050	2300	195	4	Closed
Rated power	5,000	1500	2400	255	1.5	Closed
Climb	-----	1250	2400	170	-----	Open
Take-off	-----	1850	2600	110	-----	Open

Instrumentation. - The relative location of all pressure tubes is shown in figure 3. The cooling-air pressure in front of the engine was measured by shielded total-pressure tubes on rakes (in front of four cylinders only), total-pressure tubes at the baffle entrance, and by tubes placed on the head baffle that butts against the sealing ring of the cowl. Pressures behind the engine were measured by open-end tubes in stagnant regions and by total-pressure and closed-end static-pressure tubes downstream from the cylinder. Copper tubing of 1/8-inch diameter was used for all pressure tubes; the designation, type, and exact location of the pressure tubes are given in table I. The cylinder numbering system used in the table and throughout the report is conventional; the cylinders are numbered clockwise when viewed from the rear of engine with cylinder 1 being the top rear-row cylinder.

A diagrammatic sketch of the system used for measuring the pressures is shown in figure 4. The pressures were recorded by NACA 30-cell and single-cell recording manometers and by a 100-tube liquid-manometer board photographed in flight. The 30-cell manometer consists of 30 differential-pressure cells in conjunction with selector valves and permitted an accurate recording of 254 pressures (including reference pressures) within 35 seconds. The 100-tube liquid-manometer board was connected to a two-bank, 100-tube selector valve enabling the photographing of two consecutive sets of pressures. Of these 200 pressures, 12 were used to establish the reference line for the manometer board. The reference pressure for both the 30-cell recording manometer and the 100-tube liquid manometer was the boundary-layer static pressure obtained by a flush orifice in the bottom of the fuselage.

The free-stream static pressure was measured by a calibrated swiveling static-pressure tube mounted on a boom extending 1 chord





length ahead of the right wing tip and was continuously recorded by a single-cell manometer recorder. A continuous record was also obtained of the difference between the fuselage static-orifice pressure and the free-stream static pressure. Impact pressure of the free-air stream was obtained from the record of the shielded total-pressure tube and the free-stream static-pressure tube on the wing-tip boom.

The angle of attack of the thrust axis for the level flights was obtained by measuring the inclination of the thrust axis with an inclinometer. Cowl-flap angle was obtained with a calibrated electrical position indicator. The relation between cowl-flap angle and cowl-flap exit area is shown in figure 5.

Test and analysis procedure. - The analysis of the data was accomplished by comparing runs in which all of the conditions were maintained approximately constant except for the variables being investigated. The desired conditions could not always be maintained precisely constant but the pressures were generally little affected by the variations that occurred. Various combinations of flight variables were possible by lowering the landing flaps and by extending the landing gear, thus changing the drag of the airplane. A summary of flight conditions as well as computed propeller coefficients are given in table II; figure numbers for the curves showing the test results are also included. The thrust disk-loading coefficient of the propeller  $T_c$  was computed from brake horsepower, free-stream impact pressure  $q_0$ , propeller-disk area  $S$ , and propeller efficiency  $\eta$ . Information from the Propeller Division of the Curtiss Wright Corporation was used to set up the propeller-performance curves (fig. 6) from which the propeller efficiency was determined.

In order to show the degree of stability during the flights, typical NACA pressure-cell records of free-stream impact pressure, the fuselage static-orifice pressure, and pressure altitude are shown in figure 7 for one flight run.

## RESULTS AND DISCUSSION

The discussion of the results is divided into four parts: (1) average recovery and circumferential distribution; (2) radial distribution; (3) longitudinal distribution; and (4) comparison of pressure-drop measurements. The engine cooling-air pressures presented herein are shown as a ratio of the measured pressure to free-stream impact pressure. This ratio for pressures in front of the engine will be referred to as "front recovery."





## Average Recovery and Circumferential Distribution

Effect of airplane speed. - The effect of changing airplane speed, as normally accomplished by changing engine power, on average engine cooling-air pressures (average for nine cylinders of one row) for various stations in front of and behind each of the cylinder rows with cowl flaps closed is shown in figure 8. Increased airplane speed thus obtained is accompanied by changes in other flight variables that are dependent upon the airplane and propeller-performance characteristics. The front recovery, which was relatively low as compared to wind-tunnel tests of cowlings of the same general type, increased with airplane speed; an increase in airspeed from 185 to 255 miles per hour resulted in an increase in recovery from 0.67 to 0.77. The average rear pressures were affected by increased airplane speed approximately the same as were the front recoveries, therefore making the ratio  $\Delta p/q_c$  a constant at varied airplane speed for closed cowl flaps. This trend indicates that the cooling-air weight flow would increase only slightly for this installation with an increase in front recovery.

The effect of increased airplane speed on the circumferential pressure distribution at various locations in the nacelle with cowl flaps closed is presented in figure 9. The front pressures show an improvement in the pattern with an increase in airplane speed, which results from a larger increase in the pressures on the top of the engine than at the bottom. The improvement in distribution in front of the engine as well as the increase in average pressure recovery was the combined result of changes in thrust disk-loading coefficient and angle of attack of the thrust axis, which will be discussed later. The distribution downstream of the cylinders was not noticeably affected by the increase in speed for closed cowl flaps.

Effect of cowl-flap exit area. - The front recovery was affected only slightly by increasing the cowl-flap exit area at cruising conditions although it tended to decrease in front of the rear row (fig. 10). The rear pressures showed an average decrease of about  $0.15 q_c$ , with the pressures behind the front-row barrels being least affected. Consequently, the decrease in rear pressure with an increase in cowl-flap exit area greatly increased the  $\Delta p/q_c$  ratio across the engine. This result indicates that one way to increase in cooling-air weight flow is to decrease the flow losses at the rear of the engine and from the cowl exit without changing the cowl exit area.

The effect of cowl-flap exit area upon pressure distribution is shown in figure 11. The front-row baffle-entrance pressure distribution was affected very little by opening the flaps; whereas the rear-row baffle-entrance pressures were slightly decreased on the outboard side of the engine (cylinders 3 to 9). The pressures on





the inboard side were possibly influenced by the restriction formed by the nacelle, wing, and fuselage. The distribution behind the engine was appreciably affected by opening the cowl flaps; the decrease in pressures was about 50 percent greater for the bottom cylinders in the region of the flaps than for the top cylinders. The low pressure behind the cylinders in the region of the flaps together with the relatively high front recovery for the bottom portion of the engine results in a larger pressure drop across these cylinders, even when the flaps are in the full-closed position (46 percent full-open exit area, fig. 5). This difference in cylinder cooling-air pressure drop would result in a temperature difference among cylinders for closed cowl flap, cruising operation of about  $40^{\circ}$  F, as calculated by the cooling-correlation equation established in reference 1; with the cowl flaps in full-open position a spread of approximately  $50^{\circ}$  F could be expected due to cooling-air flow distribution. From these calculations it is evident that the largest part of the temperature difference resulting from cooling-air flow distribution was caused by entrance conditions and the circumferential location of the cowl flaps, together with the fact that there was very little exit area from the cowling except through the flaps.

The effect of opening cowl flaps on cooling-air pressure recovery and distribution at a density altitude of 20,000 feet (figs. 12 and 13) was similar, in general, to that at a density altitude of 5000 feet (figs. 10 and 11) except that both the front and the rear pressures decreased slightly more at an altitude of 20,000 feet when the quantity of cooling-air flow through the engine was increased. The resulting  $\Delta p/q_c$  ratio for the various cowl-flap exit areas was, however, approximately the same for the two altitudes.

Effect of angle of attack of thrust axis. - The effect of increasing the angle of attack of the thrust axis upon pressure recovery and distribution is shown in figures 14 and 15, respectively, for closed cowl flaps. All average pressures decreased because of air spillage over the top of the cowling. The increased spillage greatly decreased the front pressure available for cooling the top cylinders. Another contributing cause of the decreased pressures at the top of the cowling was the blanketing effect of the spinner at high angles of attack of the thrust axis. This decrease in the pressures in front of the top cylinders may become more important at greater angles of attack such as are encountered in take-off, climb, or high-load conditions; in this event, the temperature distribution would be appreciably affected. The bottom pressures were less affected and in some cases were increased with increased angle of attack owing to improved entrance conditions at the bottom of the cowling. The rear pressure distribution remained essentially the same.





The flow characteristics of the cooling air into the cowling were verified by observing tufts attached in front of the engine at the entrance and on the inside of the cowling. The air flow was noted to be relatively steady in the bottom portion of the cowling and unsteady in the top portion where spillage was readily apparent. An adverse pressure gradient resulting from the abrupt break in the profile of the flow path at the rear of the spinner was indicated by tufts around the reduction-gear housing.

Effect of propeller thrust disk-loading coefficient. - The effect on cooling-air pressures of the thrust disk-loading coefficient  $T_c$ , which is indicative of the pressure rise across the propeller, is shown in figure 16. For open cowl flaps a decrease in front recovery of 0.10 resulted when the thrust disk-loading coefficient was increased 0.19. The increase in this coefficient was obtained by decreasing the impact pressure. It was concluded in reference 3, that the pressure available for cooling (cooling-air pressure drop, as used in reference 3) is a direct function of the thrust disk-loading coefficient. The increase in pressure drop with the corresponding increase in disk-loading coefficient (shown in reference 3) was largely a result of an increase in front recovery, especially for closed cowl flaps where a change of slipstream velocity has little effect on the cowl-exit pressure. The difference between the two sets of results is undoubtedly due to the differences in the respective installations. In the test installation used herein, the root section of the propeller with the cuffs appeared to be very ineffective and the nacelle-propeller diameter ratio was only 0.33. In other installations where the propeller-root section is more effective or the nacelle-propeller diameter ratio larger, an increase in thrust disk-loading coefficient would increase the pressure in front of the engine. The average rear pressures of this installation were decreased approximately the same as the front recovery, which resulted in relatively little change in the ratio  $\Delta p/q_c$  when the front recovery was changed although the cowl flaps were full open for these flights.

The pressure-distribution pattern for the cylinder heads was only slightly affected by the changes in thrust disk-loading coefficient; whereas the top front-row cylinder-barrel pressures were decreased more than other barrel pressures at the low-speed high-thrust condition (fig. 17). This decrease indicates a large adverse pressure gradient on the top of the reduction-gear housing resulting in separation from the spinner. The pressure-distribution pattern in front of the rear-row barrels was unaffected by the poor flow characteristics on top of the engine.





Effect of propeller speed. - A variation of the propeller speed and, consequently, of the advance-diameter ratio  $V/ND$  had no substantial effect upon the pressure recovery and distribution at cruising power (figs. 18 and 19), although the recovery was increased slightly at propeller speeds of 1000 to 1100 rpm. Apparently the variation in blade angle had very little effect upon the pressure available for cooling in this installation and the rotation of air behind the propeller was not sufficiently changed to affect the distribution within the cowling.

Comparison of baffle-entrance pressures on exhaust and intake sides of cylinders. - The effects of airplane speed, cowl-flap exit area, angle of attack of the thrust axis, and propeller speed on the difference between the baffle-entrance pressures on the intake and exhaust sides of the cylinder heads and barrels are shown in figure 20. The baffle-entrance pressures on the intake and exhaust side of the front-row heads and barrels were very nearly equal in all cases, indicating no appreciable change with operating conditions. The rear-row head pressures, however, were low on the exhaust side and the barrel pressures were slightly high on the exhaust side. Cowl-flap exit area was the only variable that affected these pressure differences; the spread between the pressures of the two sides was increased as the cowl flaps were opened. This effect was less noticeable for the barrels where the pressure difference was small.

#### Radial Distribution

The distribution patterns presented in the preceding section have indicated that the radial distribution of total pressure in front of the engine and of static pressure at the rear of the engine varied among cylinders; three front-row and three rear-row cylinders were selected to show this variation in the radial distribution at different locations. The locations chosen were the top of the engine, the cowl-flap region, and the bottom of the engine.

Representative plots of the radial pressure distribution at various airplane speeds, cowl-flap exit areas, and angles of attack of the thrust axis are shown in figures 21, 22, and 23, respectively. Airplane speed and angle of attack had no appreciable effect on the distribution either in front of or at the rear of the engine. Cowl-flap exit area had little effect upon the distribution upstream of the engine although it tended to become less uniform for the bottom cylinders as the cooling-air flow was increased because of the flow characteristics of the air entering the bottom of the cowling. The gradient of the static pressures behind the cylinders was increased with an increase in cowl-flap exit area, particularly for the





front-row cylinders. The difference in pressure gradients in front of and behind the individual cylinders, however, was greater than the change in gradient due to varied operating conditions.

The radial-distribution patterns indicate that distinct differences exist in the radial pressure distribution between the front- and rear-row cylinders. In this particular installation, the entrance pressures for the front-row cylinders were highest near the middle of the cylinder; whereas, for the rear-row cylinders the pressure was lowest near the middle with exception of the bottom cylinders where more stable flow into the cowling prevailed. The pressure distribution behind the engine cylinders was affected largely by the circumferential location of the cowl flaps as indicated by the large pressure gradient in the cowl-flap region.

When changes occur in the radial pressure distribution of a given installation or when like engines are placed in different nacelles that do not have the same radial distribution, the different engine air-flow conductivities and consequently the different mass-flow pressure-drop relations that will result are important considerations.

#### Longitudinal Distribution

The relations between the useful pressure drop across the cylinders and the entrance and exit losses of the cylinders have been indirectly shown by the patterns of circumferential and radial pressure distribution. These relations are, however, more conveniently shown by plots of longitudinal distribution of pressure through the engine. Such curves are presented in figures 24 and 25 for closed and open cowl-flap positions, respectively. The distribution at three circumferential locations around the engine and the average distribution are included. The total pressures ahead of the cylinders are those measured by tubes at the baffle entrance. These tubes (on all front-row cylinders) were used for the pressures ahead of the engine and indicated pressures of approximately the same magnitudes as the shielded tubes in front of four cylinders of the engine. The use of these tubes prevented determination of the baffle-entrance losses to the front-row cylinders but these losses were undoubtedly small. The pressures directly behind the cylinders were measured by total-pressure tubes rather than static-pressure tubes in order that the exit losses might be evaluated. The rear-most pressures behind the engine were measured by static-pressure tubes behind the intake pipes where the velocity pressure was small; the differences between this pressure and the front-row baffle-entrance pressure is considered to be the total pressure drop across the engine installation.

Faint, illegible text in the left column, possibly bleed-through from the reverse side of the page.

Faint, illegible text in the right column, possibly bleed-through from the reverse side of the page.

Faint, illegible text in the left column, possibly bleed-through from the reverse side of the page.

Faint, illegible text in the right column, possibly bleed-through from the reverse side of the page.



For closed cowl flaps the longitudinal distribution through the engine is similar at each of the three circumferential locations because it is chiefly dependent on the absolute value of pressure drop across any particular region of the engine (fig. 24). On the assumption that the baffle-entrance losses are negligible, the average pressure drops across the front-row heads and barrels were 55 and 40 percent of the total pressure drop across the engine, respectively. The baffle-exit losses made up the remaining portion of the total. In the rear row, the entrance loss for both the heads and the barrels was about 20 percent of the total; the drops across the heads and barrels were 65 and 50 percent of the total, respectively, and the exit losses were 15 and 30 percent, respectively. From a comparison of the two rows, it is noted that, regardless of the rear-row entrance losses, the useful pressure drop across the rear row is roughly 20 percent greater than that across the front row. This difference in useful pressure drop across the two rows, if it is assumed to be a reliable indication of distribution of cooling-air weight flow, would result in the front-row cylinders running  $10^{\circ}$  to  $30^{\circ}$  F hotter than the rear-row cylinders, dependent upon operating conditions. For an engine that develops a greater amount of power in the front row than in the rear row, as reported by the Army Air Forces in 1943 (Memo. Rep. Ser. No. 57-503-858), this cooling-air flow distribution between rows could be of considerable detriment to efficient operation.

The longitudinal distribution for open cowl flaps is shown in figure 25. The distribution between the front and rear row is very nearly the same as for closed flaps (fig. 24); the difference between the head and barrel pressure drops, however, became slightly larger when the flaps were opened.

#### Comparison of Pressure-Drop Measurements

A large number of different types of pressure tube at various locations have been used in test-stand, wind-tunnel, and flight tests as an index of cooling-air flow through an air-cooled engine. The location of many of the pressure tubes was duplicated in the present tests enabling a comparison of pressure-drop measurements. This comparison may be used to facilitate correlation of various cooling investigations that have employed different methods of measuring pressure drop. The results are tabulated in table III by listing the various pressure-drop recoveries for open and closed cowl flaps and by showing the relation between the different pressure drops by comparing them with the pressure drop used in reference 1 ( $\Delta p_1$ ). The table includes two general types of cooling-air pressure-drop measurement. Methods 1 to 5 show the difference



The results of the study are presented in Table 1. The data show that the mean value of the variable 'X' is significantly higher than the mean value of the variable 'Y'. This difference is statistically significant at the 5% level. The standard deviation of 'X' is also higher than that of 'Y'. The correlation coefficient between 'X' and 'Y' is positive and significant. The regression equation is  $Y = 0.8X + 1.2$ . The coefficient of determination is 0.75, indicating that 75% of the variance in 'Y' is explained by 'X'. The residuals are normally distributed with a mean of zero and a standard deviation of 1.5. The overall fit of the model is good, as indicated by the high R-squared value.

### Discussion of the Results

The results of the study are consistent with the theoretical expectations. The positive correlation between 'X' and 'Y' suggests that as 'X' increases, 'Y' also tends to increase. The regression equation provides a clear relationship between the two variables. The high coefficient of determination indicates that the model is a good fit for the data. The normal distribution of the residuals supports the use of linear regression. The findings have important implications for the field of study. Further research is needed to explore the underlying mechanisms of the relationship between 'X' and 'Y'. The study also highlights the need for more data to improve the accuracy of the model.

between average entrance pressure of front-row cylinders and average exit pressure of rear-row cylinders; this type of measurement includes the losses in the entrance passages to the rear-row cylinders and in the exit passages from the front-row cylinders. Methods 6 to 9 show the difference between the average entrance and exit pressures of the individual cylinders, thereby excluding the entrance- and exit-passage losses. As shown in table III, a large difference exists among the various pressure-drop measurements. Across the heads, the largest indicated pressure drop is almost twice as great as the smallest one; whereas across the barrels, the difference is larger. The relation between the various pressure drops for this installation was little affected by the cowl-flap position, although opening the cowl flaps increased the value of the  $\Delta p/q_c$  ratio roughly 60 percent. The large differences in the values of pressure drop obtained by different methods of measurement and the effect of different installations on engine cooling-air distribution indicates that good correlation of the cooling results of like engines in different installations cannot be expected unless the instrumentation and installation differences are taken into account.

Because of the difficulty in accurately measuring cooling-air weight flow in a flight investigation, a qualitative comparison of the reliability of the various pressure-drop methods was impossible, even though large differences among the various measurements were shown. The pressure-drop method used in reference 1 ( $\Delta p_1$ ) gave the best total engine cooling correlation; however, this comparison is dependent on the accuracy of the correlation procedure in accounting for differences in cooling variables other than cooling-air weight flow. Consequently, this procedure is not considered sufficiently conclusive for making a qualitative comparison of pressure-drop measurements.

#### SUMMARY OF RESULTS

From the flight investigation of the engine cooling-air pressure recovery and distribution of a two-row radial engine enclosed in a low-inlet-velocity cowl, the following results were obtained:

1. The average front pressure recovery, which was relatively low for this engine installation, increased with an increase in airplane speed during normal level flight.

2. The pressure drops across the front-row cylinder heads and barrels for closed cowl flaps were 55 and 40 percent, respectively,





of the difference between the pressures front and rear of the engine; the pressure drops across the rear-row heads and barrels were 65 and 50 percent, respectively.

3. The static pressures behind the heads were lower than those behind the barrels; this difference increased when the cowl flaps were opened, especially for the front-row cylinders in the cowl-flap region. This change in radial distribution with operating conditions was smaller than the difference between individual cylinders.

4. The pressure distribution in front of the engine had little effect upon the distribution behind the engine; however, an increase in average front pressure recovery resulted in almost as large an increase in average rear pressure.

5. A change in pressure at the rear of the engine accomplished by varying the cowl-flap area had little effect on the pressure recovery and distribution in front of the engine.

6. The general pattern of the circumferential distribution behind the engine was chiefly determined by the circumferential location of the cowl flaps.

7. An increase in angle of attack of the thrust axis decreased the front recovery at the top of the engine because of spillage from the cowling and separation from the spinner; the air flow into the bottom of the cowling remained relatively steady.

8. An increase in propeller thrust disk-loading coefficient decreased the average front recovery for this installation.

9. The speed of the propeller had little effect upon the pressure recovery and no effect on the distribution at cruising power.

10. Large differences, sometimes amounting to 100 percent, were obtained among the results indicated by various methods of measuring pressure drop across the engine.

#### CONCLUDING REMARKS

The results of these tests indicate that an important consideration in the design of cowlings and cowl flaps should be the obtaining of good distribution of cooling air as well as minimum drag for the installation; the results further show that the cooling-air flow distribution and, consequently, the temperature-limited performance of a given engine installation is considerably affected by cowl-entrance conditions and circumferential location of the cowl flaps.



The fact that these tests showed that the front recovery decreased with an increase in propeller thrust disk-loading coefficient provides additional evidence that the recovery is greatly affected by the combined propeller-nacelle design. Also of significance is that a large increase in front recovery resulted in a similar increase in rear pressure, indicating that an increase in the front recovery of an air-cooled engine is not always an effective method of increasing the cooling-air weight flow.

Aircraft Engine Research Laboratory,  
National Advisory Committee for Aeronautics,  
Cleveland, Ohio, December 3, 1945.

#### REFERENCES

1. Bell, E. Barton, Morgan, James E., Disher, John H., and Mercer, Jack R.: Flight Investigation of the Cooling Characteristics of a Two-Row Radial Engine Installation. I - Cooling Correlation. NACA TN No. 1092, 1946.
2. Pinkel, Benjamin: Heat-Transfer Processes in Air-Cooled Engine Cylinders. NACA Rep. No. 612, 1938.
3. Stickle, George W., Naiman, Irven, and Crigler, John L.: Pressure Available for Cooling with Cowling Flaps. NACA Rep. No. 720, 1941.



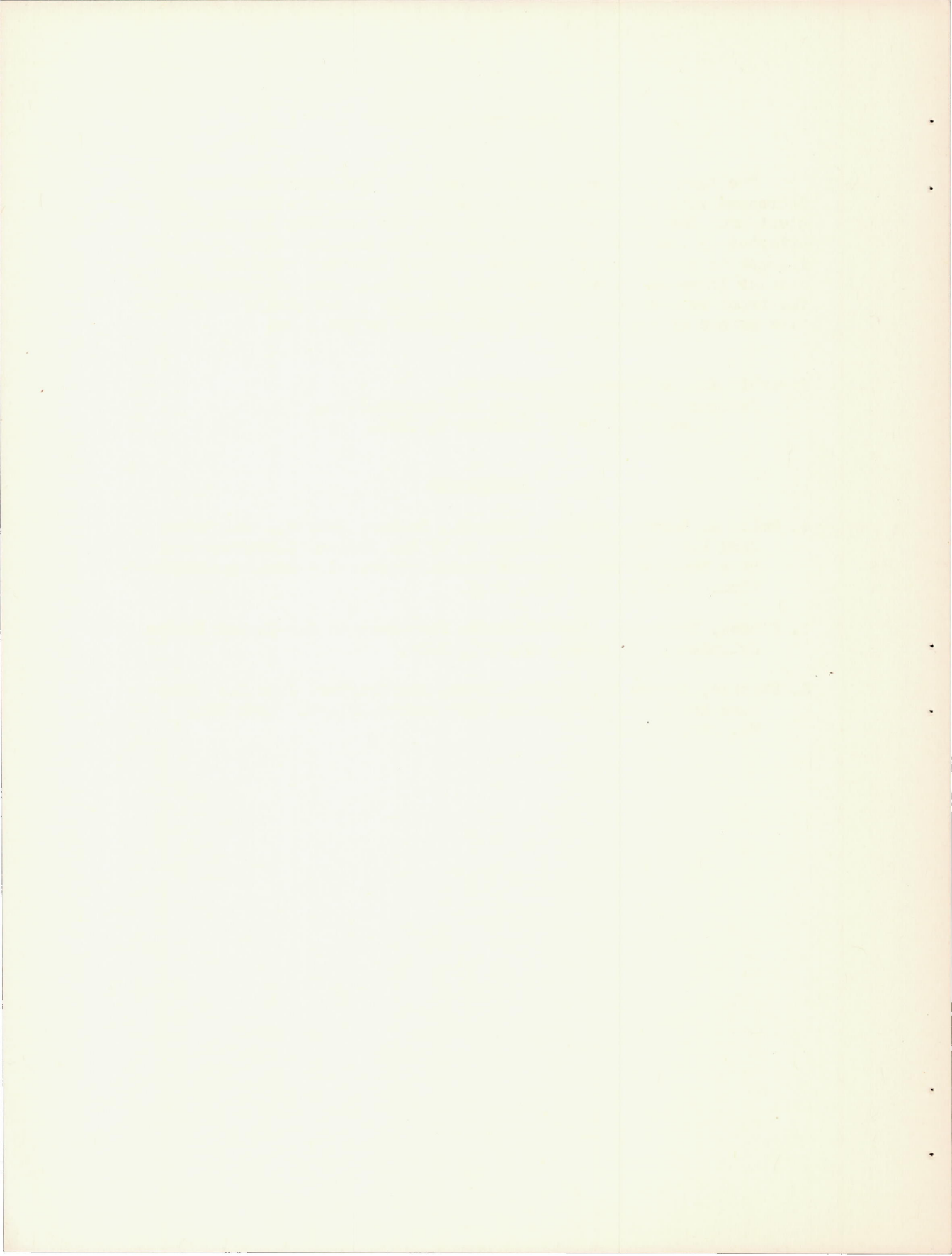


TABLE I - ENGINE COOLING-AIR PRESSURE-TUBE INSTALLATION

NACA TN No. 1109

Pressure tube (a)	Relative location	Type	Circumferential location		Axial location (in.)	Radial location from cylinder-flange base (in.)
			Cylinders	Position relative to cylinder		
H <sub>h1</sub>	Front of head on rake	Shielded total head	2,6,11,16	Center of cylinder	$5\frac{5}{8}$ upstream of front-row baffle entrance	$7\frac{5}{8}$
H <sub>b1</sub>	Front of barrel on rake	---do---	---do---	---do---	---do---	$4\frac{1}{8}$
H <sub>h21</sub>	Between fin and baffle at head-baffle entrance	Total head	All	Intake side	$3\frac{1}{16}$ downstream of baffle-entrance curl	$7\frac{13}{16}$
H <sub>h2t</sub>	---do---	---do---	---do---	Center of cylinder	---do---	$12\frac{7}{8}$
H <sub>h2e</sub>	---do---	---do---	1,4,5,7,8,10,11,14,15,17,18	Exhaust side	---do---	$7\frac{13}{16}$
H <sub>b21</sub>	Between fin and baffle at barrel-baffle entrance	---do---	All	Intake side	---do---	$3\frac{3}{16}$
H <sub>b2e</sub>	---do---	---do---	1,4,5,7,8,10,11,14,15,17,18	Exhaust side	---do---	$3\frac{3}{16}$
H <sub>h3</sub>	Front of cowl sealing ring	Baffle tap	1,7,13	Center of cylinder	On baffle butting against sealing ring	$14\frac{1}{4}$
H <sub>h4</sub>	Rear of head on rake	Total head	All	---do---	$7\frac{5}{8}$ downstream of head fins	$7\frac{5}{8}$
P <sub>h4</sub>	---do---	Closed-end static	---do---	---do---	---do---	7
H <sub>b4</sub>	Rear of barrel on rake	Total head	---do---	---do---	$7\frac{5}{8}$ downstream of barrel fins	$4\frac{1}{2}$
P <sub>b4</sub>	---do---	Closed-end static	---do---	---do---	---do---	$3\frac{7}{8}$
P <sub>h5</sub>	Behind cowl sealing ring	Open-end static	---do---	---do---	$1\frac{1}{8}$ behind head sealing baffle	$15\frac{3}{4}$
P <sub>b6</sub>	Rear of barrel between flange and fins	---do---	---do---	---do---	$1\frac{1}{16}$ behind cylinder barrel	$5\frac{5}{8}$
P <sub>h7</sub>	Downstream of engine (heads)	---do---	Rear row	In baffle-exit curl, intake side	At baffle exit	$7\frac{13}{16}$
P <sub>b7</sub>	Downstream of engine (barrels)	---do---	---do---	---do---	---do---	$3\frac{3}{16}$
P <sub>h8</sub>	Downstream of engine	Closed-end static	5,11,17	Behind charge-air intake pipe	2 behind intake pipe	$10\frac{1}{4}$

<sup>a</sup>See figure 3 for explanation of symbols and subscripts.

TABLE II - SUMMARY OF FLIGHT CONDITIONS AND COMPUTED PROPELLER COEFFICIENTS

17

Figure	Airplane conditions					Engine conditions		Propeller coefficients		
	Density of free air (slug/cu ft)	Pressure altitude (ft)	Impact pressure (in. water)	Angle of attack of thrust axis (deg)	Cowl-flap angle (deg)	Brake horsepower	Engine speed (rpm)	Speed-power coefficient $C_s$	Advance-diameter ratio V/ND	Thrust disk-loading coefficient $T_c$
8,9, 20,21	0.00205	3453	16.6	4.5	Closed	783	2400	1.878	1.066	0.102
	.00206	3494	22.0	3.3	---do---	1012	2392	2.057	1.230	.087
	.00205	3710	28.9	1.7	---do---	1267	2400	2.210	1.380	.072
	.00204	4994	33.1	1.5	---do---	1549	2416	2.301	1.489	.072
10,11, 20,22	0.00206	3178	22.8	2.7	Closed	1008	2408	2.083	1.240	0.082
	.00206	3198	21.8	2.6	14.5	1017	2414	2.036	1.210	.089
	.00206	3188	20.6	3.7	27.0	1019	2420	1.981	1.175	.097
	.00206	3208	19.7	3.6	Open	1024	2420	1.934	1.148	.104
12,13	0.00129	18257	14.8	5.1	Closed	823	2420	2.001	1.255	0.101
	.00126	18322	15.7	4.5	15.0	916	2400	2.052	1.320	.103
	.00127	18289	14.3	5.0	30.8	916	2400	1.959	1.261	.119
	.00127	18240	14.1	5.1	Open	916	2400	1.950	1.250	.121
14,15, 20,23	0.00207	3422	22.3	0.9	Closed	1011	2400	2.053	1.230	0.085
	.00206	3494	22.0	3.3	---do---	1012	2392	2.057	1.230	.087
	.00206	4820	18.6	5.1	---do---	804	2414	1.981	1.123	.088
16,17	0.00207	5080	10.2	3.7	Open	1025	2410	1.275	0.681	0.274
	.00206	5112	14.0	1.8	---do---	1023	2406	1.621	.970	.175
	.00206	5133	17.0	1.8	---do---	1024	2408	1.792	1.072	.131
	.00206	5176	22.4	3.1	---do---	1023	2404	2.055	1.232	.086
18,19, 20	0.00206	3886	21.7	3.4	Closed	1013	1806	2.273	1.610	0.089
	.00205	3886	21.5	3.4	---do---	1010	1996	2.117	1.457	.087
	.00205	3886	21.8	3.4	---do---	1017	2200	2.204	1.387	.088
	.00205	3886	22.3	3.1	---do---	1020	2398	2.063	1.234	.089
	.00205	3886	20.8	3.4	---do---	1009	2584	1.933	1.105	.087
24	0.00206	3178	22.8	2.7	Closed	1008	2408	2.083	1.240	0.082
25	0.00206	3208	19.7	3.6	Open	1024	2420	1.934	1.148	0.104

NATIONAL ADVISORY  
COMMITTEE FOR AERONAUTICS

NACA TN No. 1109

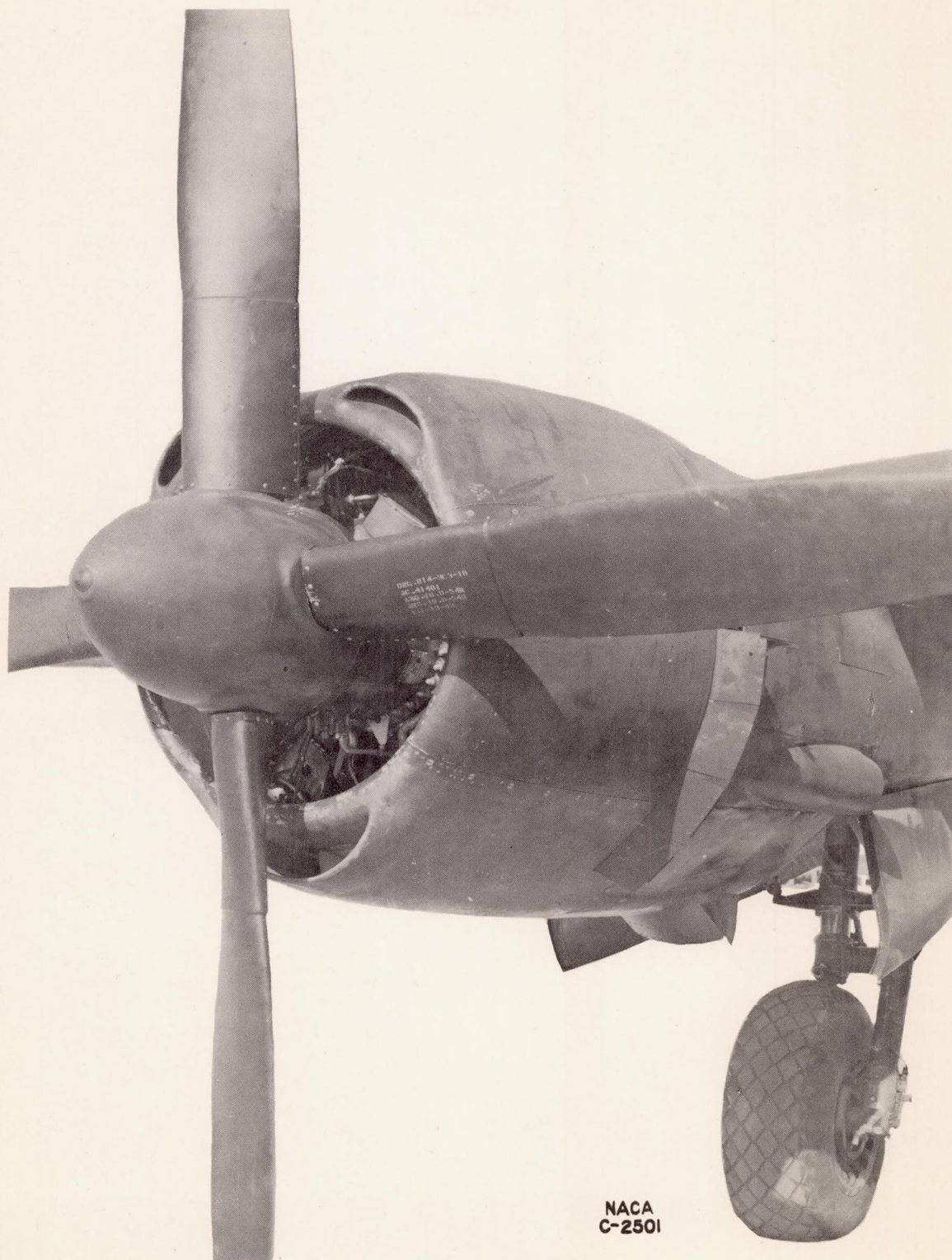


TABLE III - COMPARISON OF VARIOUS PRESSURE-DROP MEASUREMENTS  
[Altitude, 5000 ft]

Δp	Pressure-drop method	Δp/q <sub>c</sub>		Δp/Δp <sub>1</sub>	
		Cowl flaps closed	Cowl flaps full open	Cowl flaps closed	Cowl flaps full open
Head					
a <sub>1</sub>	$\left(\frac{H_{h21} + H_{h2t}}{2}\right)_{fr} - (P_{h4})_{rr}$	0.28	0.45	1.00	1.00
2	$\left(\frac{H_{h21} + H_{h2t}}{2}\right)_{fr} - (P_{h5})_{rr}$	0.33	0.50	1.18	1.11
3	$\left(\frac{H_{h21} + H_{h2t}}{2}\right)_{fr} - (P_{h7})_{rr}$	0.29	0.45	1.04	1.00
4	$\left(\frac{H_{h21} + H_{h2t}}{2}\right)_{fr} - \left(\frac{P_{h5} + P_{h7}}{2}\right)_{rr}$	0.31	0.48	1.11	1.07
5	$\left(\frac{H_{h21} + H_{h2t}}{2}\right)_{fr} - (H_{h4})_{rr}$	0.25	0.42	0.89	0.93
6	$\left(\frac{H_{h21} + H_{h2t}}{2}\right)_{ae} - (P_{h4})_{ae}$	0.22	0.34	0.79	0.76
7	$\left(\frac{H_{h21} + H_{h2t}}{2}\right)_{ae} - (P_{h5})_{ae}$	0.30	0.46	1.07	1.02
8	$\left(\frac{H_{h21} + H_{h2t}}{2}\right)_{ae} - (H_{h4})_{ae}$	0.18	0.30	0.64	0.67
9	<sup>b</sup> H <sub>h1</sub> - P <sub>h4</sub> <sub>ae</sub>	0.24	0.37	0.86	0.82
Barrel					
a <sub>1</sub>	H <sub>b21</sub> <sub>fr</sub> - P <sub>b4</sub> <sub>rr</sub>	0.24	0.40	1.00	1.00
2	H <sub>b21</sub> <sub>fr</sub> - P <sub>b6</sub> <sub>rr</sub>	0.26	0.42	1.08	1.05
3	H <sub>b21</sub> <sub>fr</sub> - P <sub>b7</sub> <sub>rr</sub>	0.27	0.43	1.12	1.07
4	H <sub>b21</sub> <sub>fr</sub> - $\left(\frac{P_{b6} + P_{b7}}{2}\right)_{rr}$	0.26	0.42	1.08	1.05
5	H <sub>b21</sub> <sub>fr</sub> - H <sub>b4</sub> <sub>rr</sub>	0.17	0.31	0.71	0.77
6	H <sub>b21</sub> <sub>ae</sub> - P <sub>b4</sub> <sub>ae</sub>	0.16	0.27	0.67	0.68
7	H <sub>b21</sub> <sub>ae</sub> - P <sub>b6</sub> <sub>ae</sub>	0.16	0.26	0.67	0.65
8	H <sub>b21</sub> <sub>ae</sub> - H <sub>b4</sub> <sub>ae</sub>	0.10	0.19	0.42	0.48
9	<sup>b</sup> H <sub>b1</sub> - P <sub>b4</sub> <sub>ae</sub>	0.19	0.30	0.79	0.75

<sup>a</sup>Pressure-drop method used in reference 1.  
<sup>b</sup>Front of cylinders 2, 6, 11, and 16 only.





NACA  
C-2501

Figure 1. - Test-engine installation.





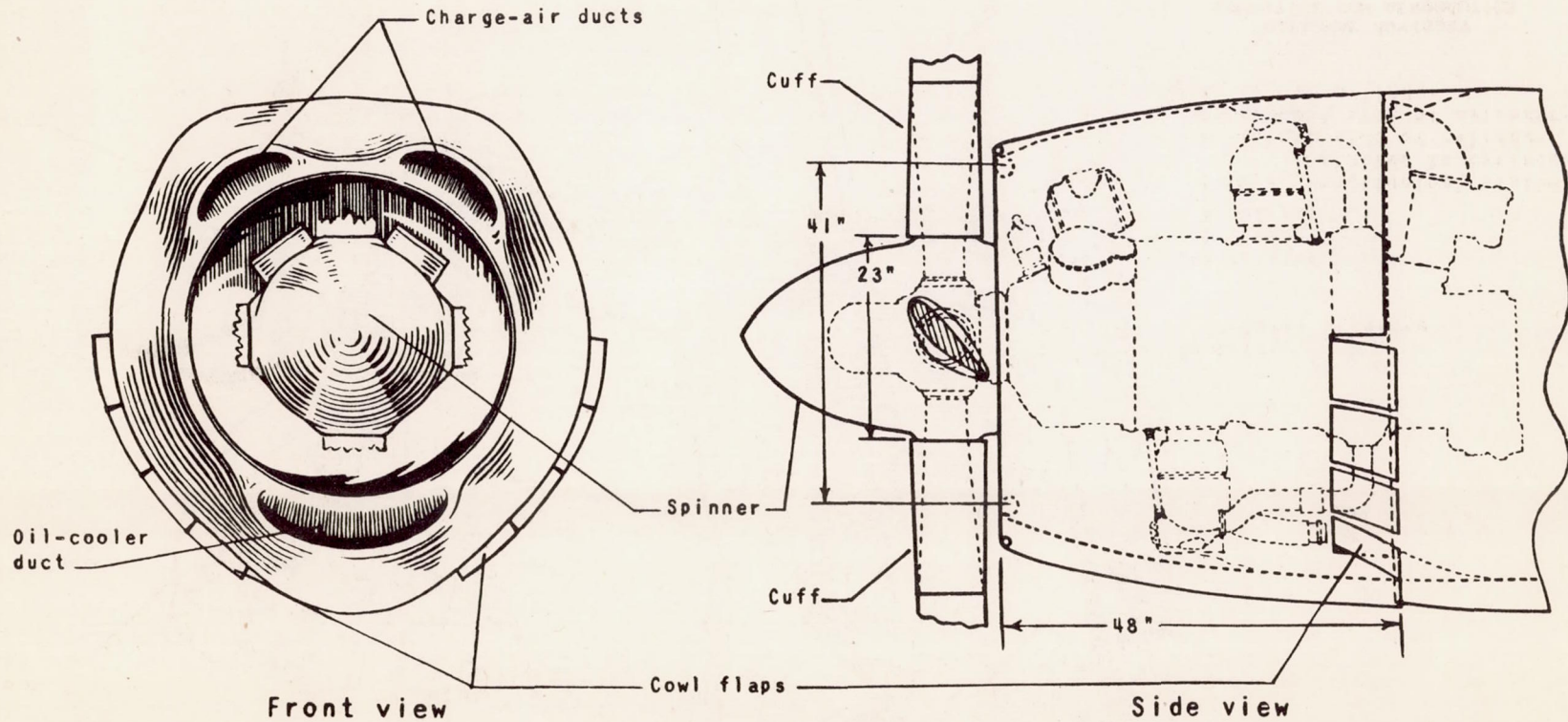


Figure 2. - Sketch of low-inlet-velocity cowling and propeller spinner and cuffs.

NATIONAL ADVISORY  
COMMITTEE FOR AERONAUTICS

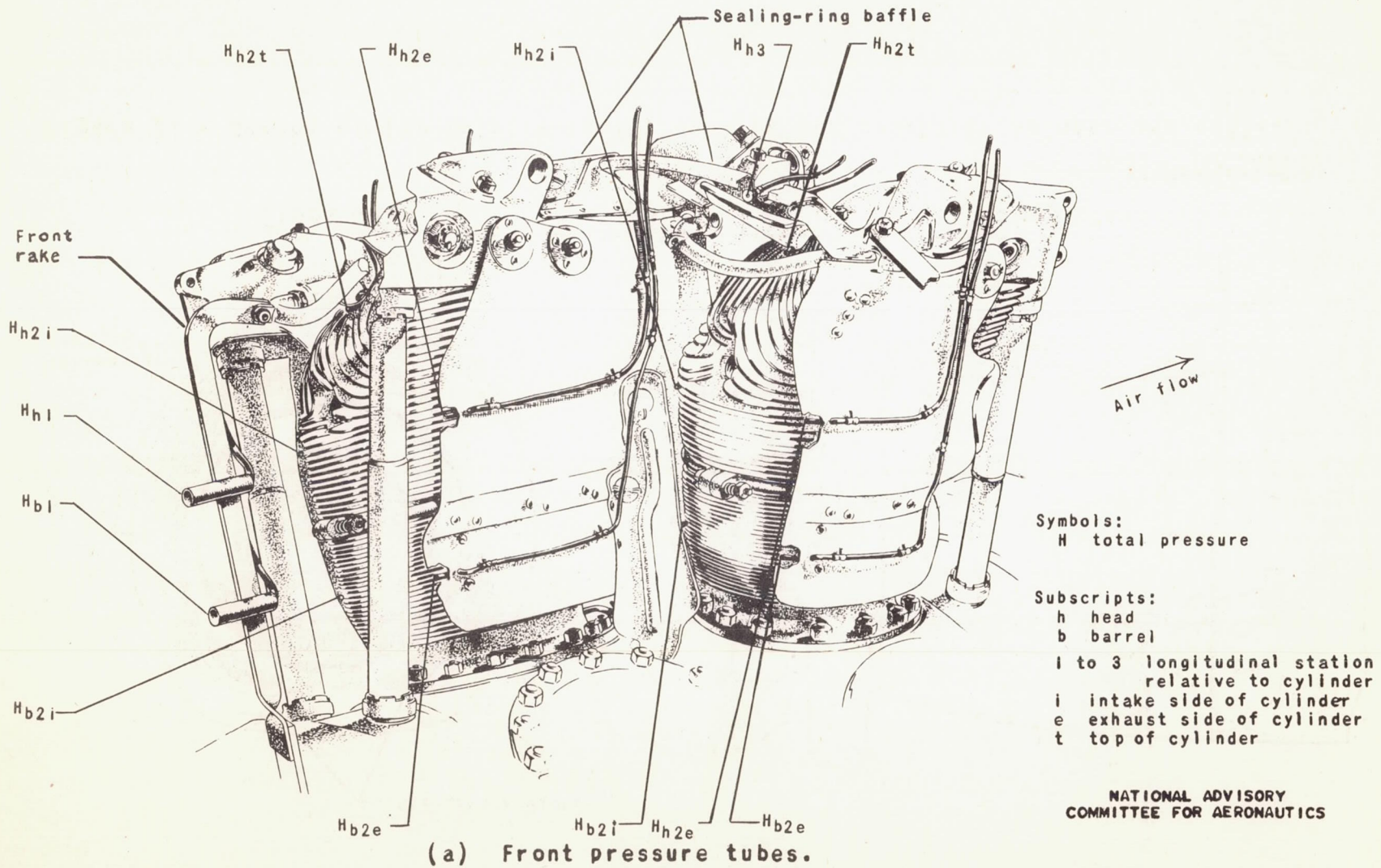
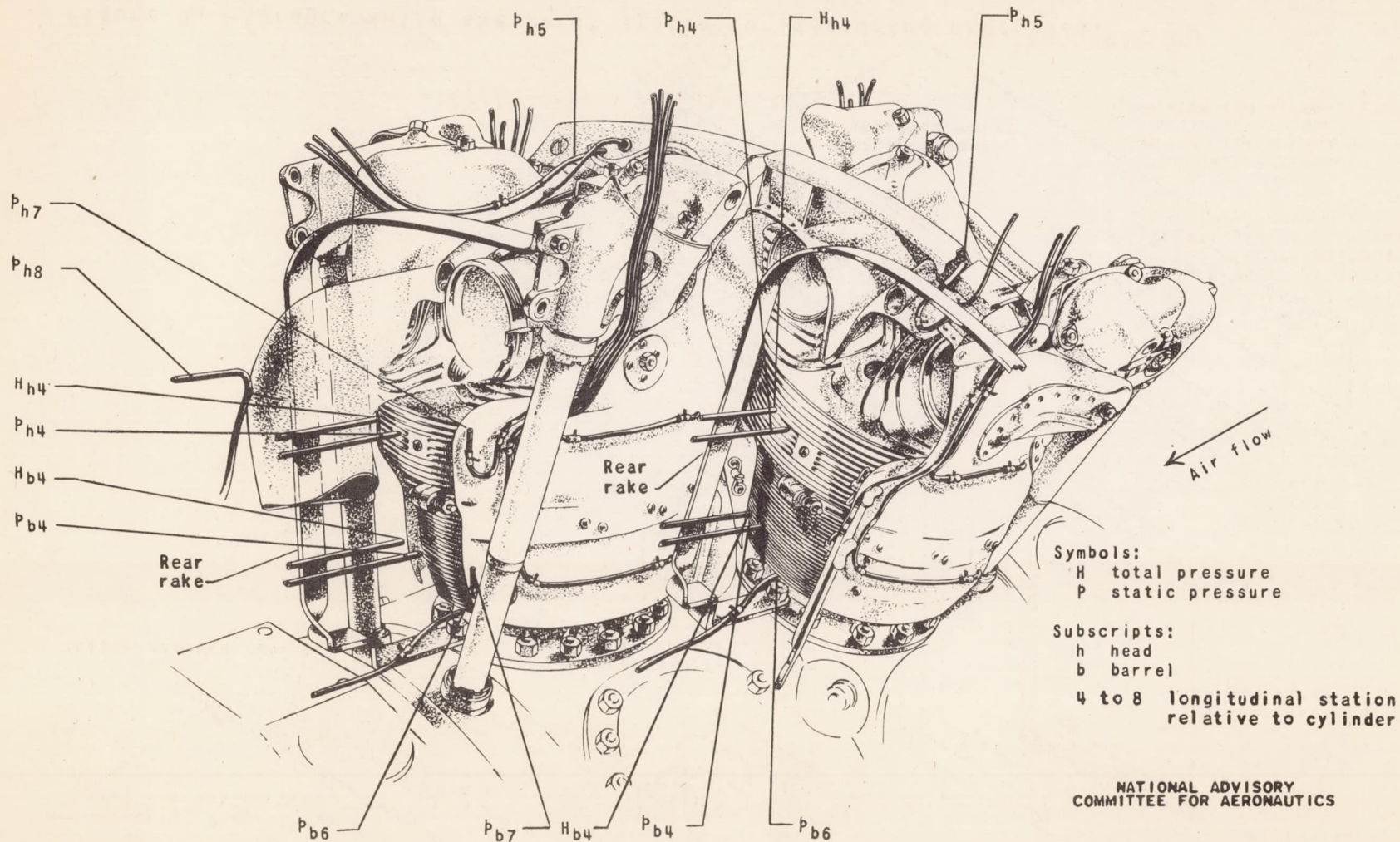


Figure 3. - Front- and rear-row cylinders showing pressure-tube installation.

£b





(b) Rear pressure tubes.

Figure 3. - Concluded. Front- and rear-row cylinders showing pressure tube installation.

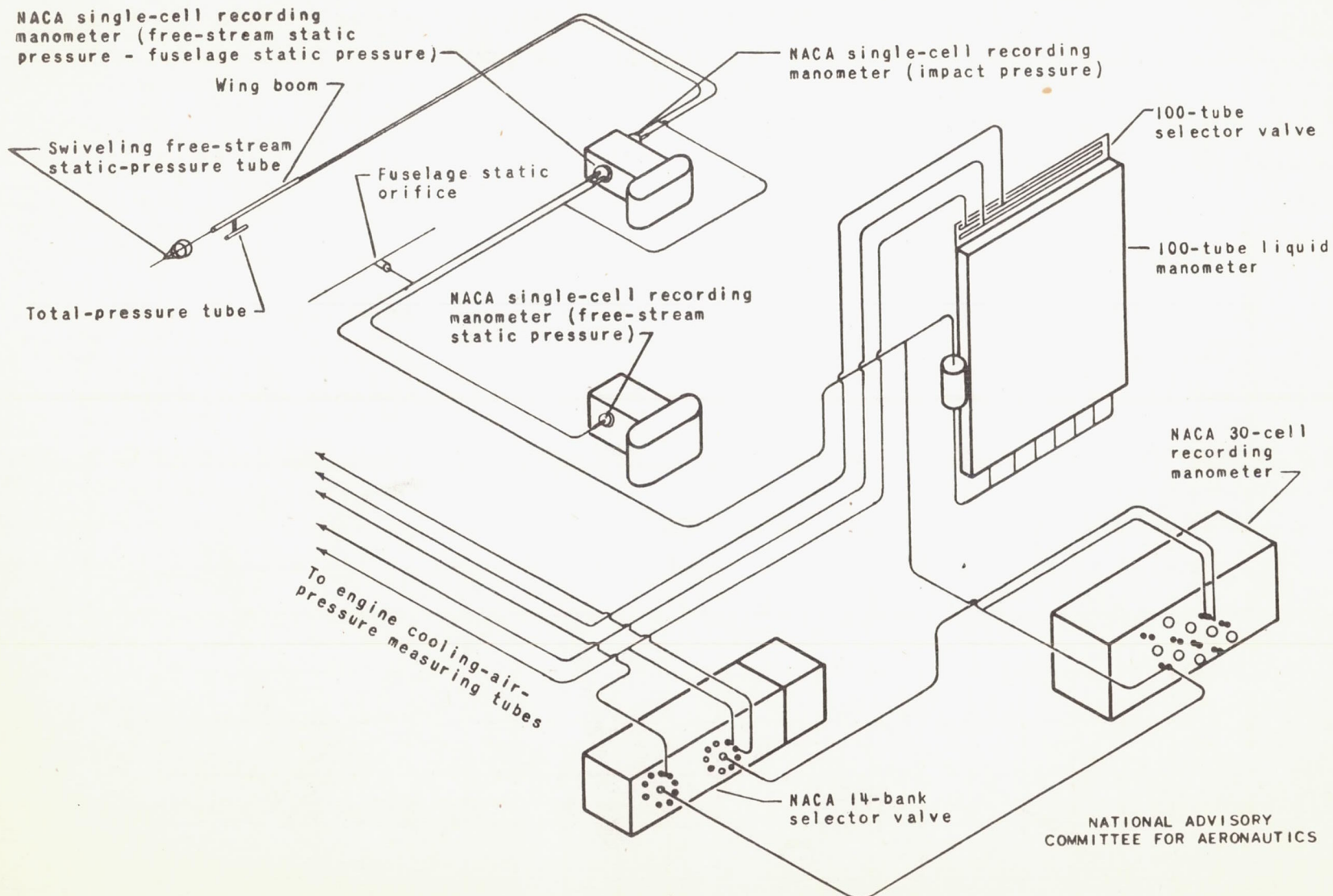


Figure 4. - Diagrammatic sketch of system for measuring pressures.



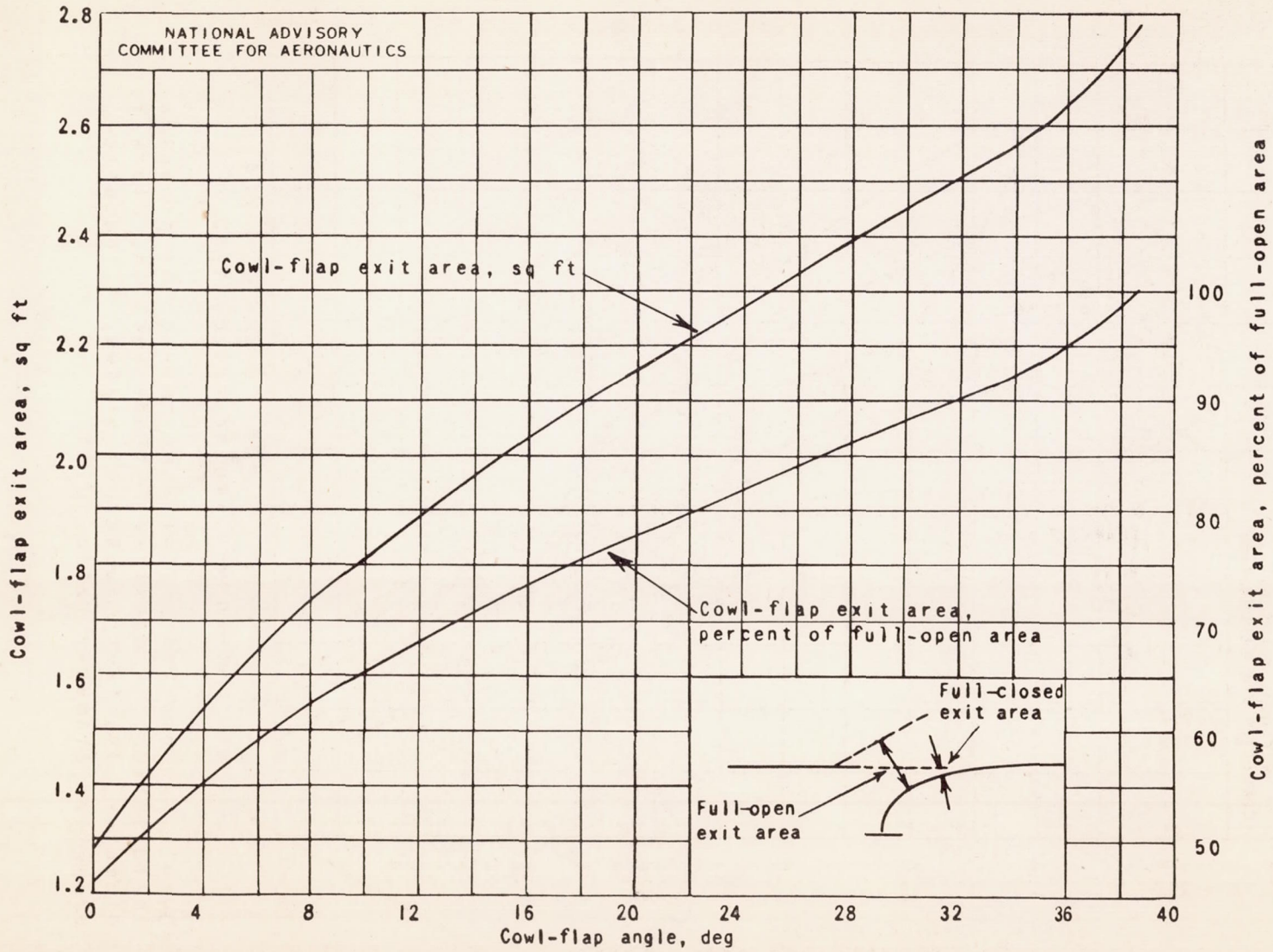


Figure 5. - Relation between cowl-flap angle and exit area.



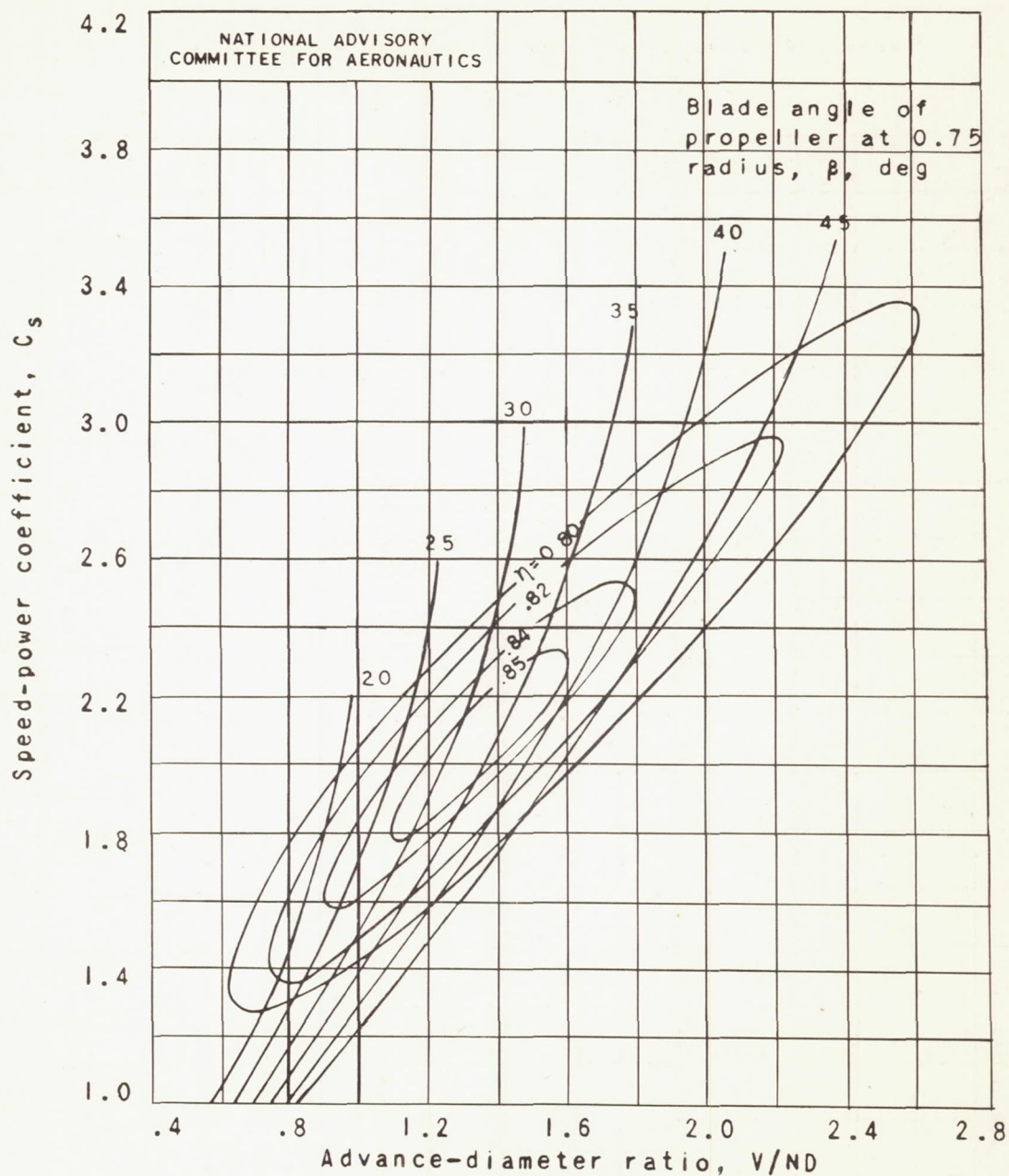


Figure 6. - Computed performance curves for propeller installation. Propellers: blade section, Clark Y; diameter, 13½ feet; number of blades, 4; nacelle-propeller diameter ratio, 0.33.

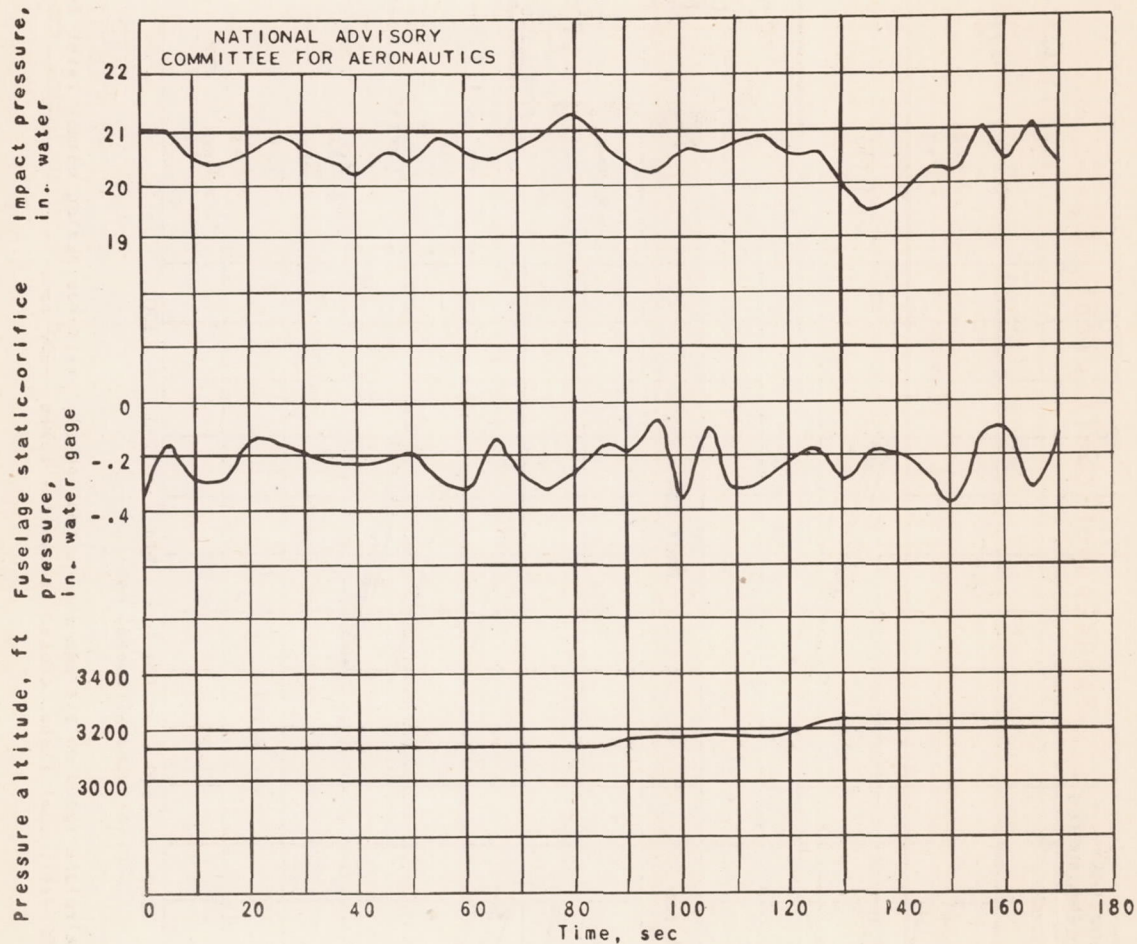


Figure 7. - Typical record of free-stream impact pressure, fuselage static-orifice pressure, and pressure altitude.

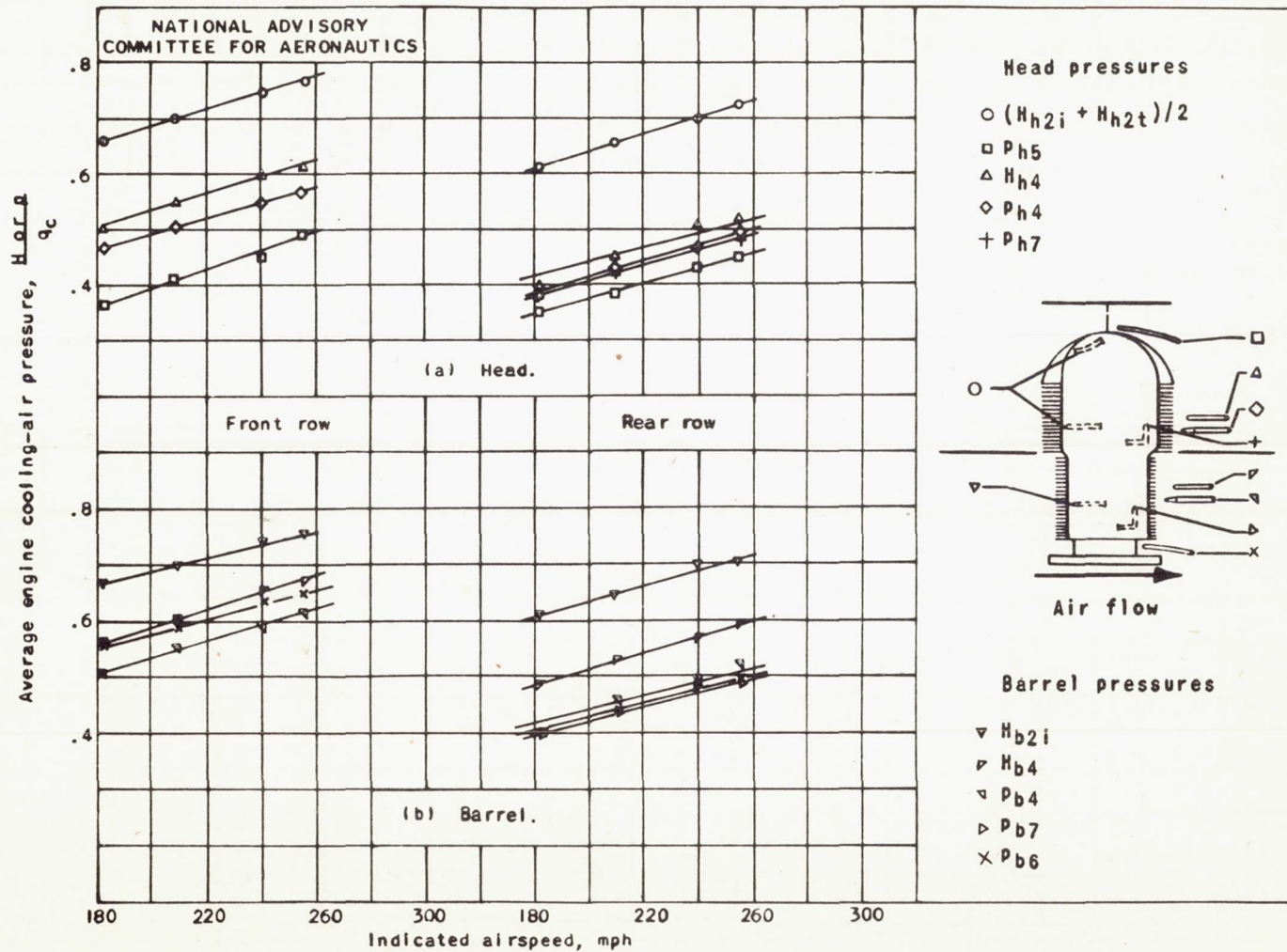


Figure 8. - Effect of airplane speed on average engine cooling-air pressures during normal level flight. Density altitude, 5000 feet; cowl flaps, closed; propeller speed, 1200 rpm.



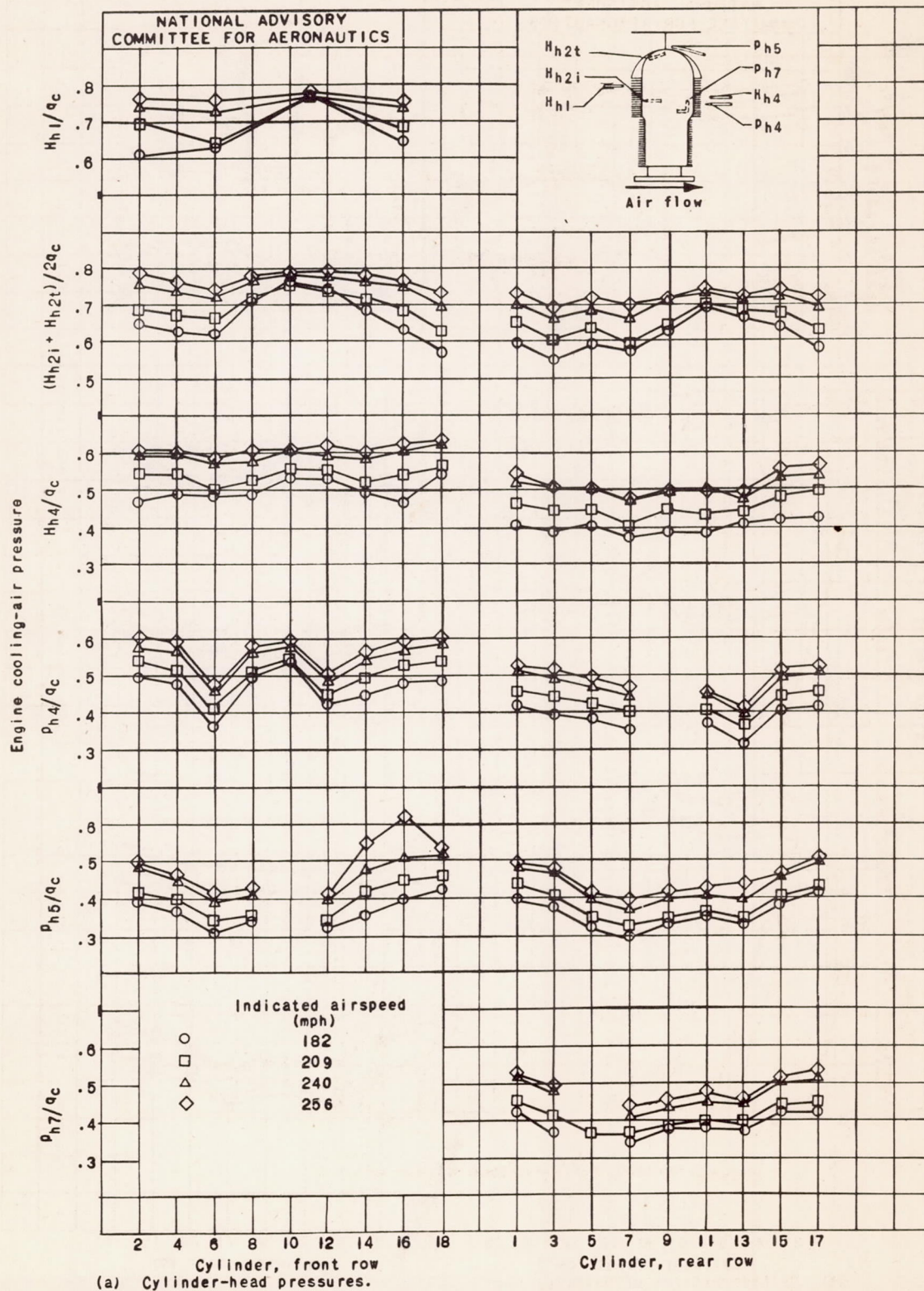


Figure 9. - Effect of airplane speed on circumferential pressure distribution during normal level flight. Density altitude, 5000 feet; cowl flaps, closed; propeller speed, 1200 rpm.

Fig. 9b

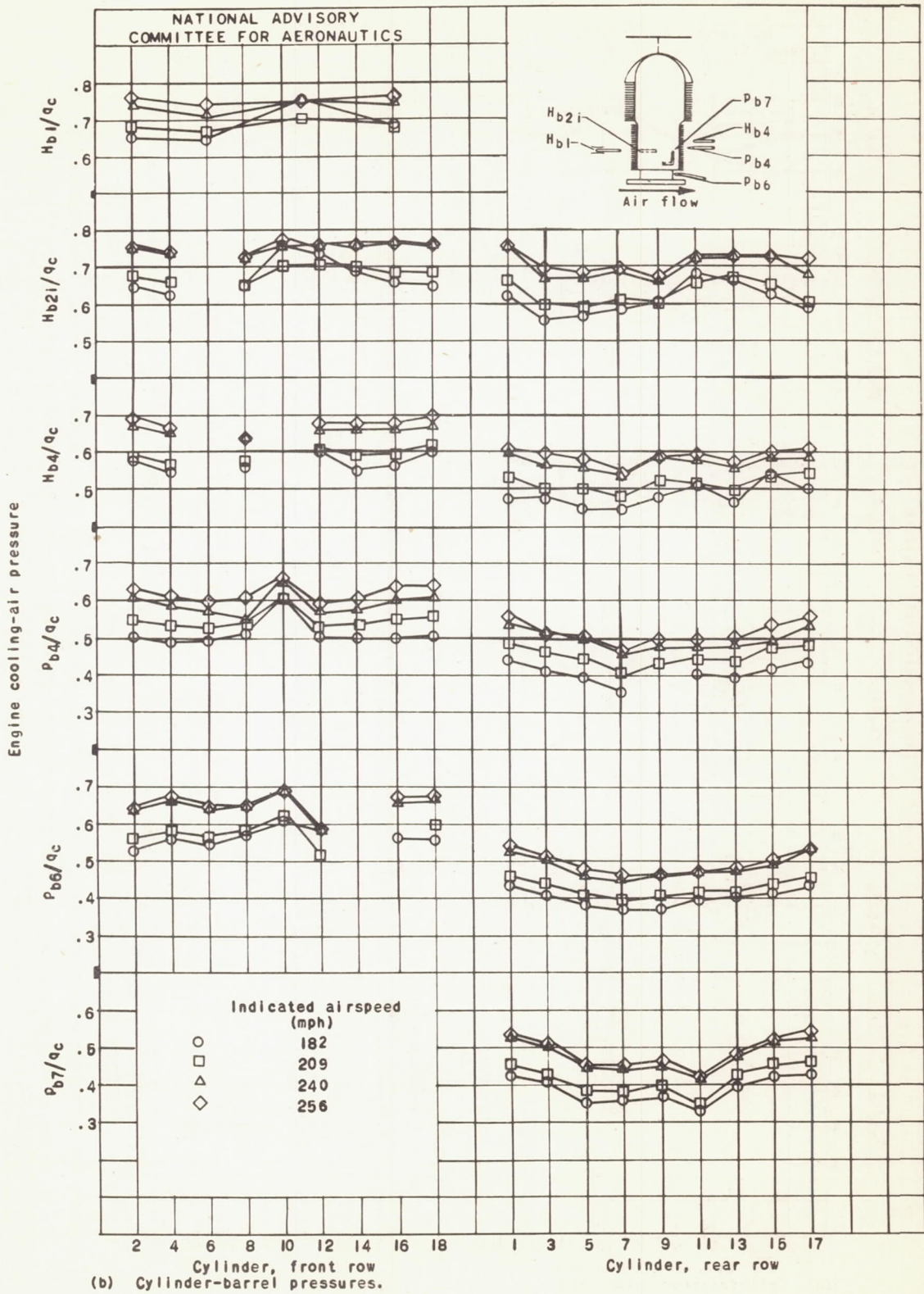


Figure 9. - Concluded. Effect of airplane speed on circumferential pressure distribution during normal level flight. Density altitude, 5000 feet; cowl flaps closed; propeller speed, 1200 rpm.



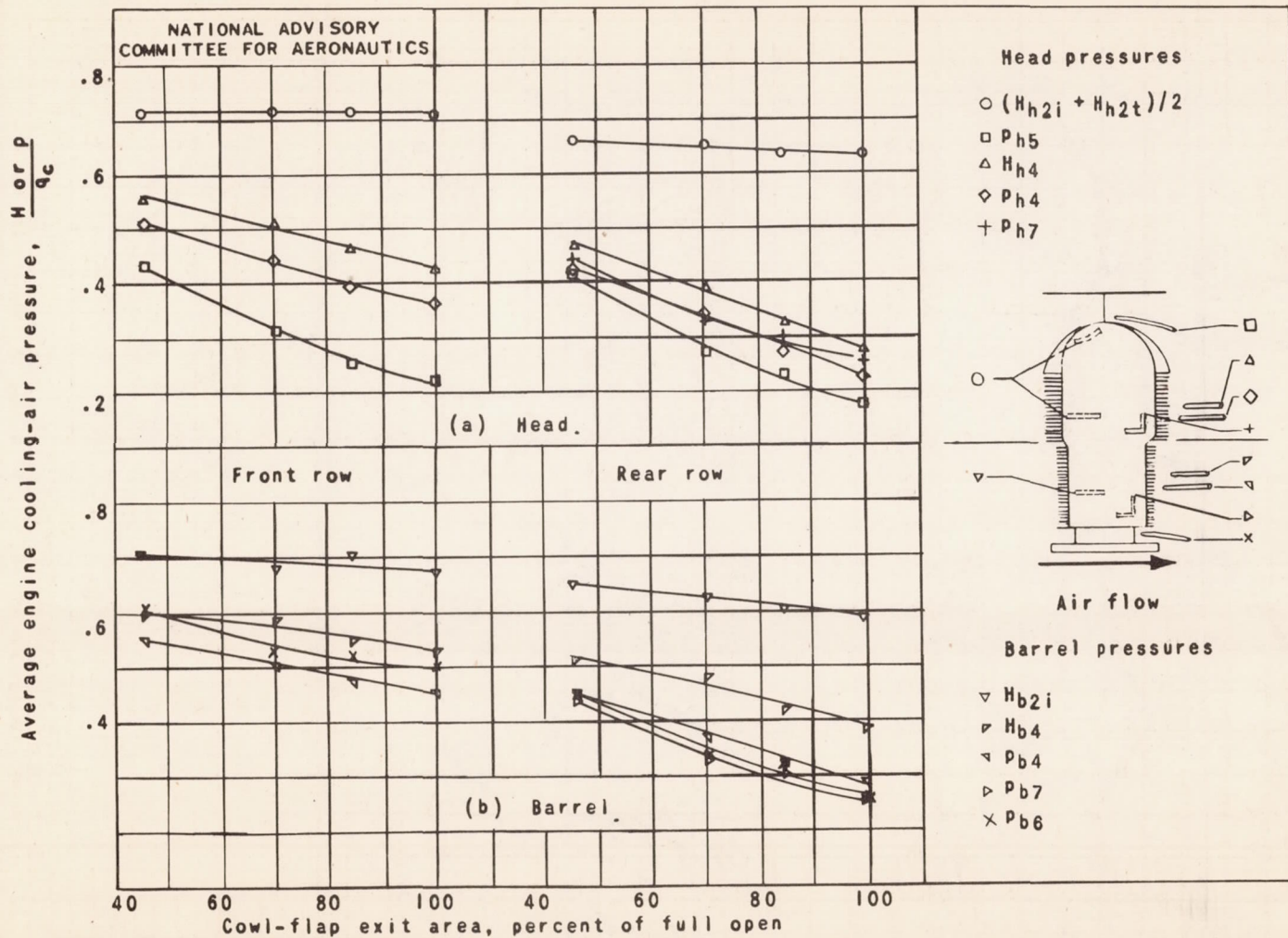


Figure 10. - Effect of cowl-flap exit area on average engine cooling-air pressures. Density altitude, 5000 feet; free-stream impact pressure, 20 to 23 inches water; angle of attack of thrust axis,  $2.6^\circ$  to  $3.7^\circ$ ; thrust disk-loading coefficient 0.08 to 0.10; propeller speed, 1200 rpm.



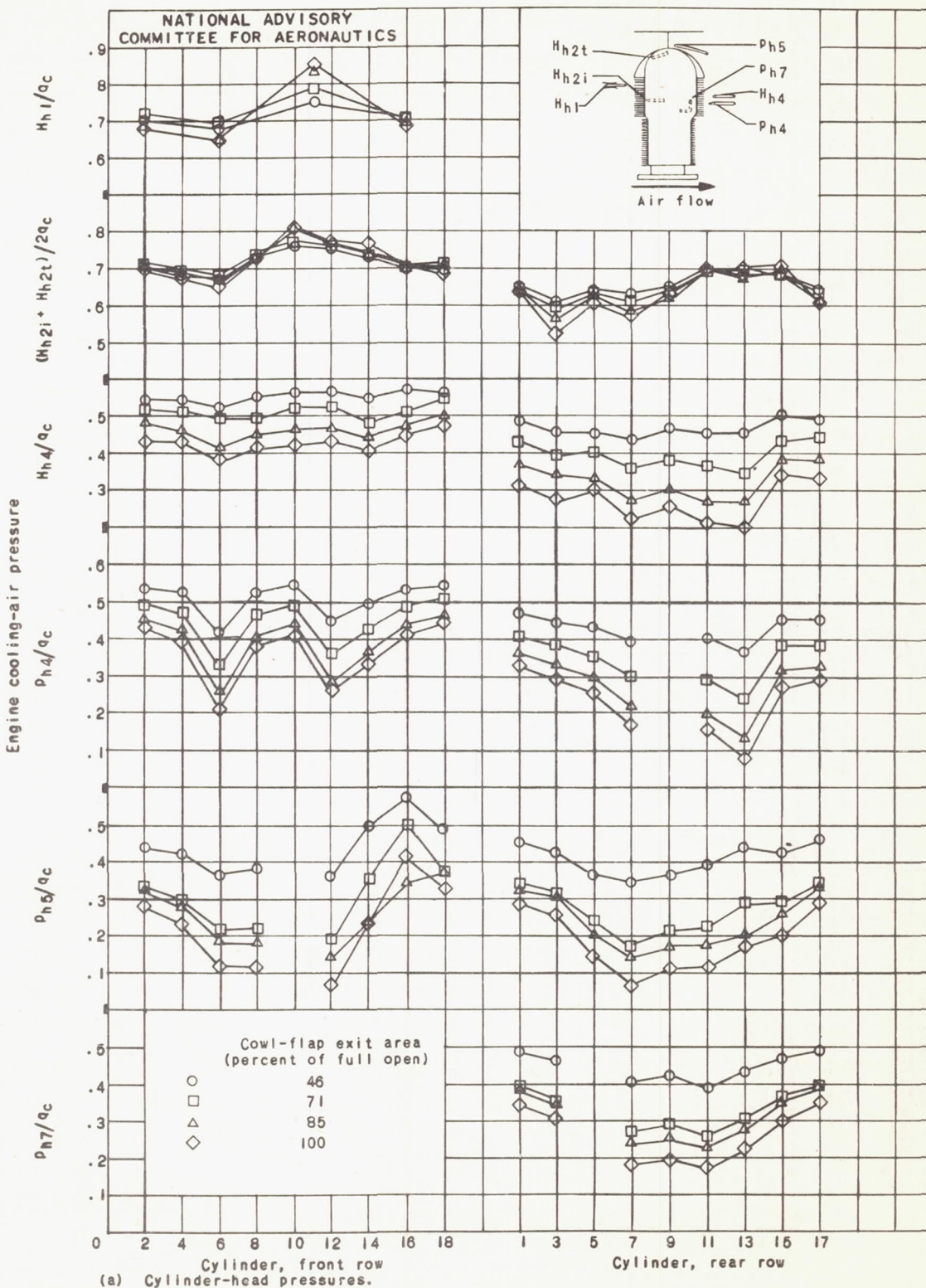


Figure 11. - Effect of cowl-flap exit area on circumferential pressure distribution. Density altitude, 5000 feet; free-stream impact pressure, 20 to 23 inches water; angle of attack of thrust axis, 2.6° to 3.7°; thrust disk-loading coefficient, 0.08 to 0.10; propeller speed, 1200 rpm.

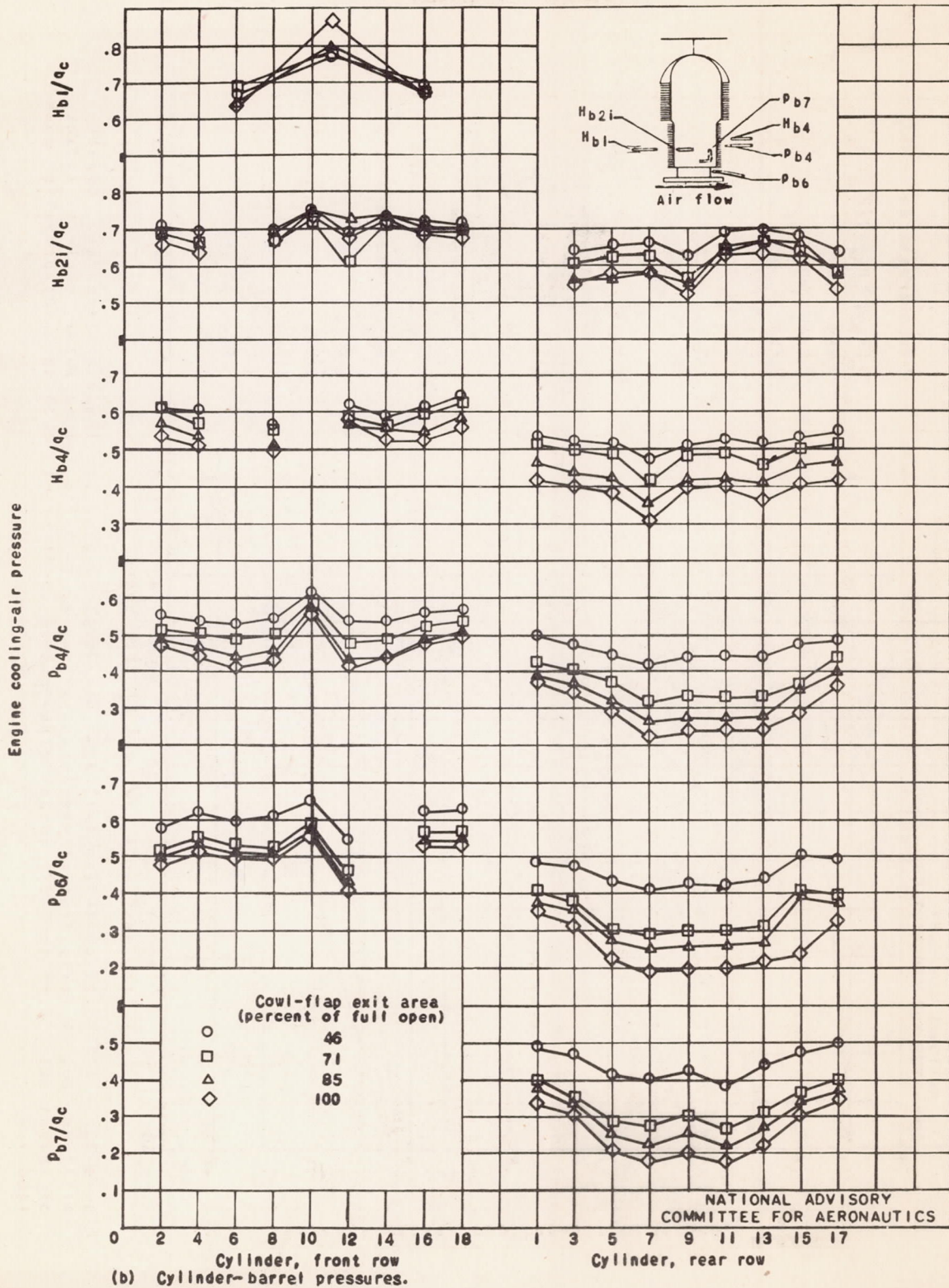


Figure 11. - Concluded. Effect of cowl-flap exit area on circumferential pressure distribution. Density altitude, 5000 feet; free-stream impact pressure, 20 to 23 inches water; angle of attack of thrust axis,  $2.6^{\circ}$  to  $3.7^{\circ}$ ; thrust disk-loading coefficient, 0.08 to 0.10; propeller speed, 1200 rpm.



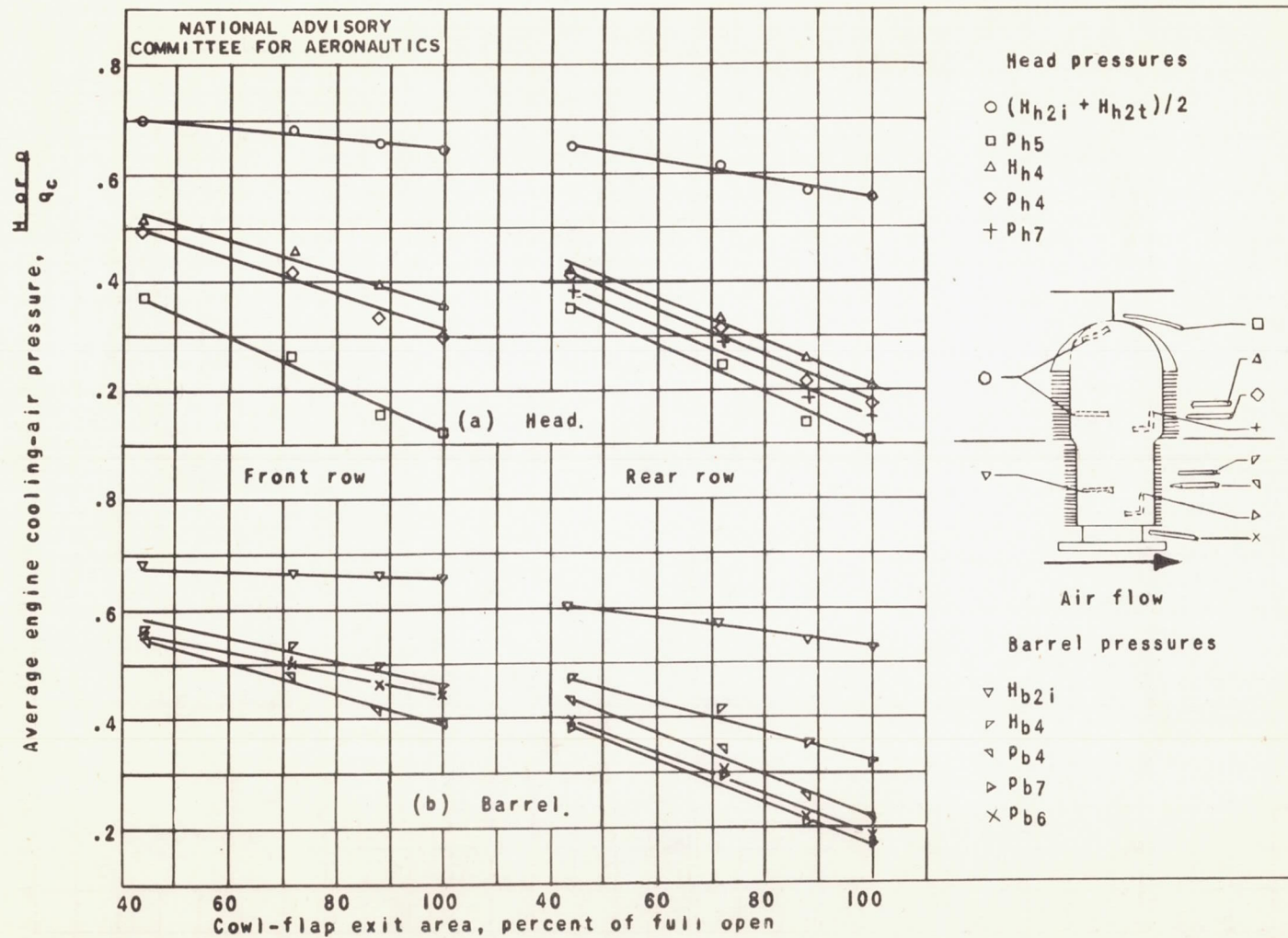


Figure 12. - Effect of cowl-flap exit area on average engine cooling-air pressures. Density altitude, 20,000 feet; free-stream impact pressure, 14 to 16 inches water; angle of attack of thrust axis,  $4.5^\circ$  to  $5.1^\circ$ ; thrust disk-loading coefficient, 0.10 to 0.12; propeller speed, 1200 rpm.



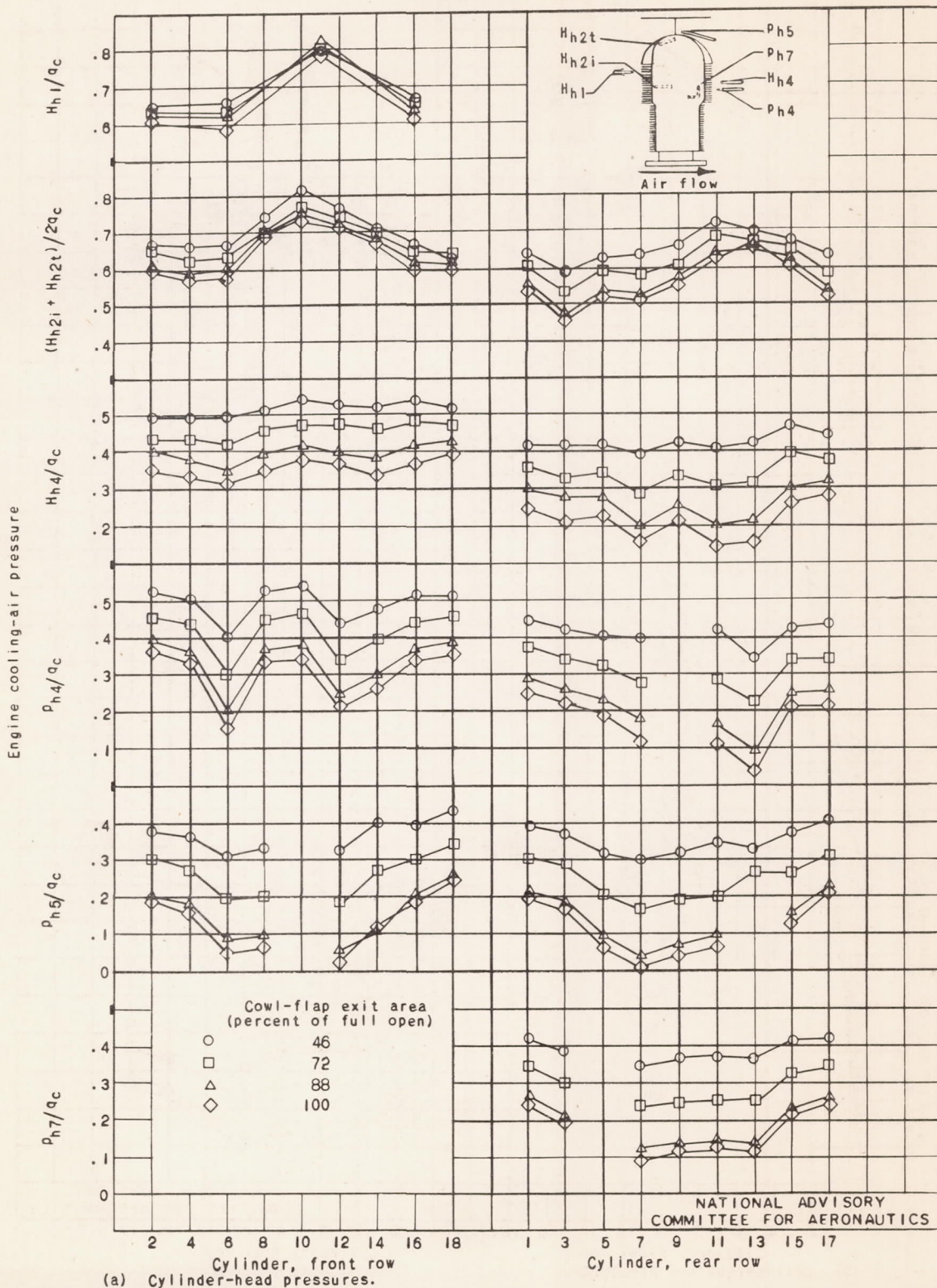
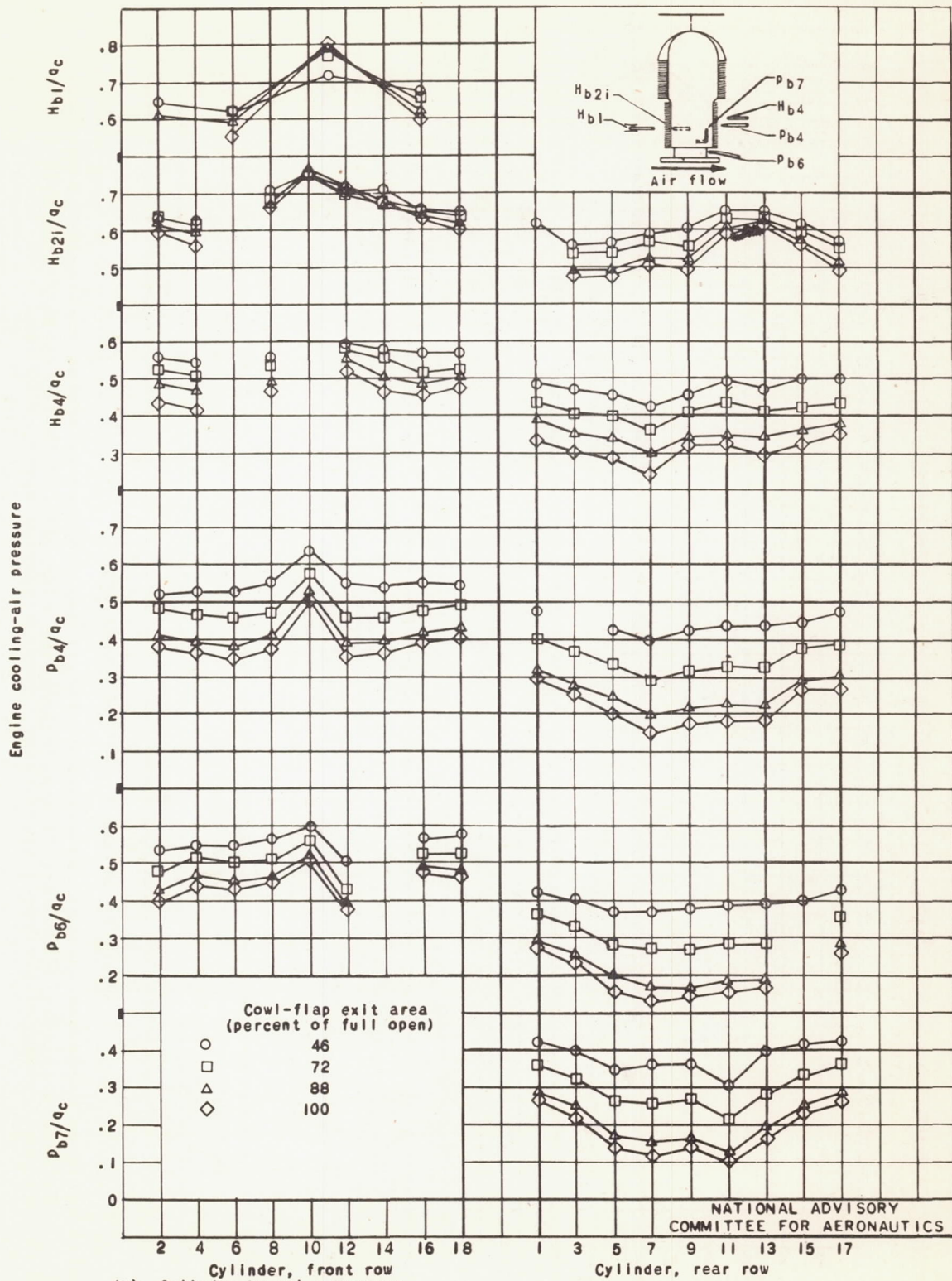


Figure 13. - Effect of cowl-flap exit area on circumferential pressure distribution. Density altitude, 20,000 feet; free-stream impact pressure, 14 to 16 inches water; angle of attack of thrust axis, 4.5° to 5.1°; thrust disk-loading coefficient, 0.10 to 0.12; propeller speed 1200 rpm.

Fig. 13b



(b) Cylinder-barrel pressures.

Figure 13. - Concluded. Effect of cowl-flap exit area on circumferential pressure distribution. Density altitude, 20,000 feet; free-stream impact pressure, 14 to 16 inches water; angle of attack of thrust axis,  $4.5^\circ$  to  $5.1^\circ$ ; thrust disk-loading coefficient, 0.10 to 0.12; propeller speed 1200 rpm.



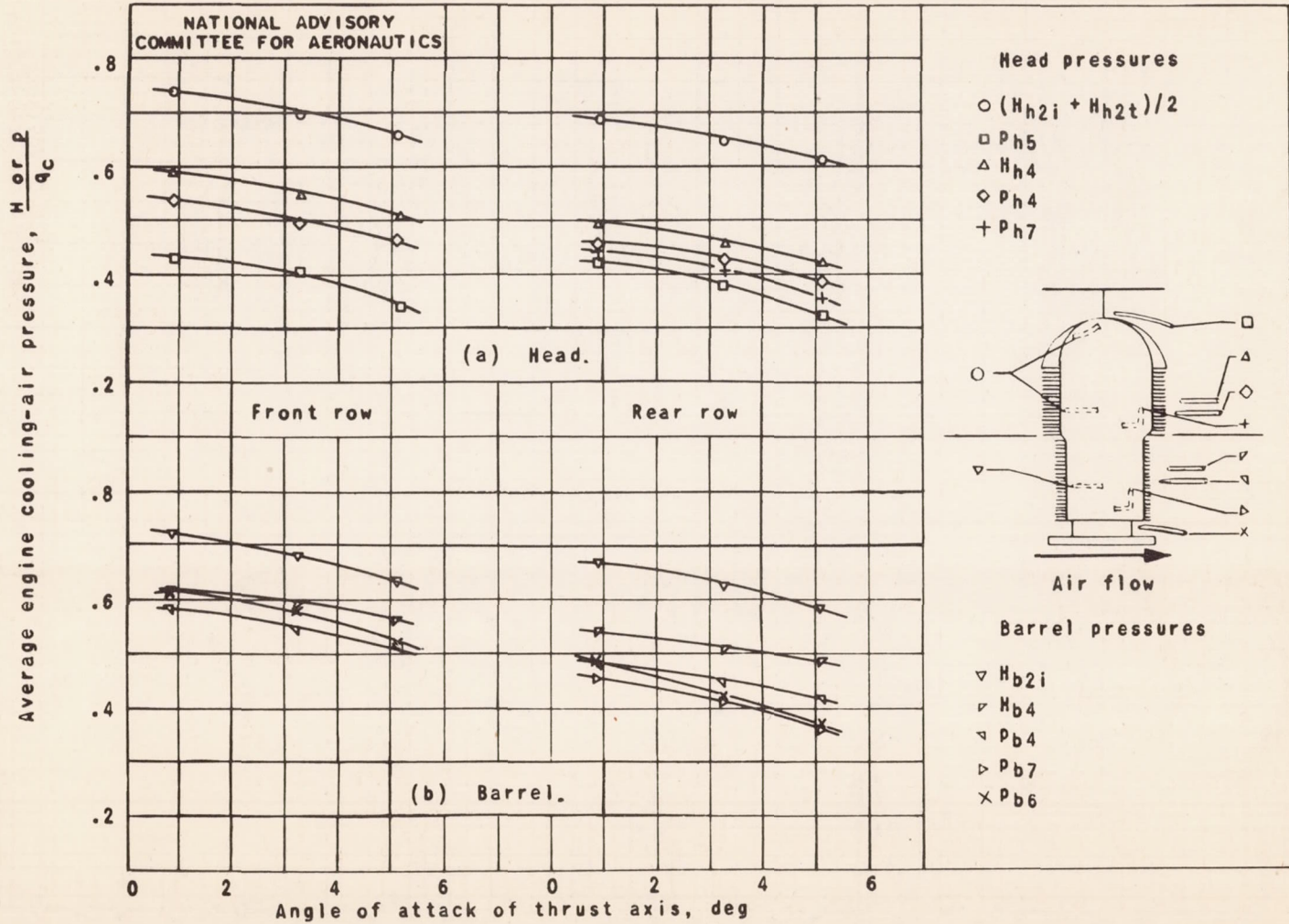


Figure 14. - Effect of angle of attack of thrust axis on average engine cooling-air pressures. Density altitude, 5000 feet; free-stream impact pressure, 19 to 22 inches water; cowl flaps, closed; thrust disk-loading coefficient, 0.09; propeller speed, 1200 rpm.



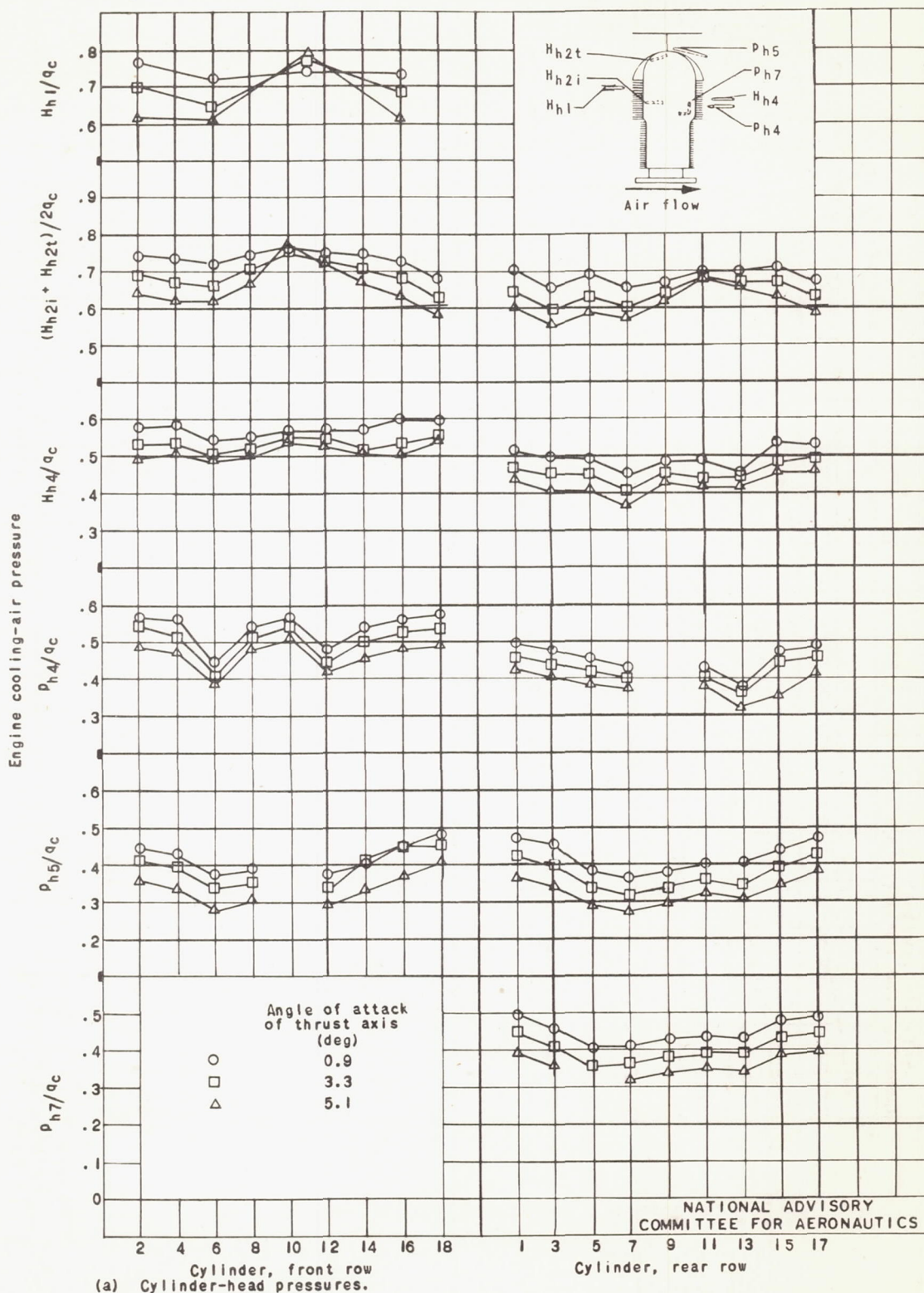


Figure 15. - Effect of angle of attack of thrust axis on circumferential pressure distribution. Density altitude, 5000 feet; free-stream impact pressure, 19 to 22 inches water; cowl flaps, closed; thrust disk-loading coefficient, 0.09; propeller speed, 1200 rpm.

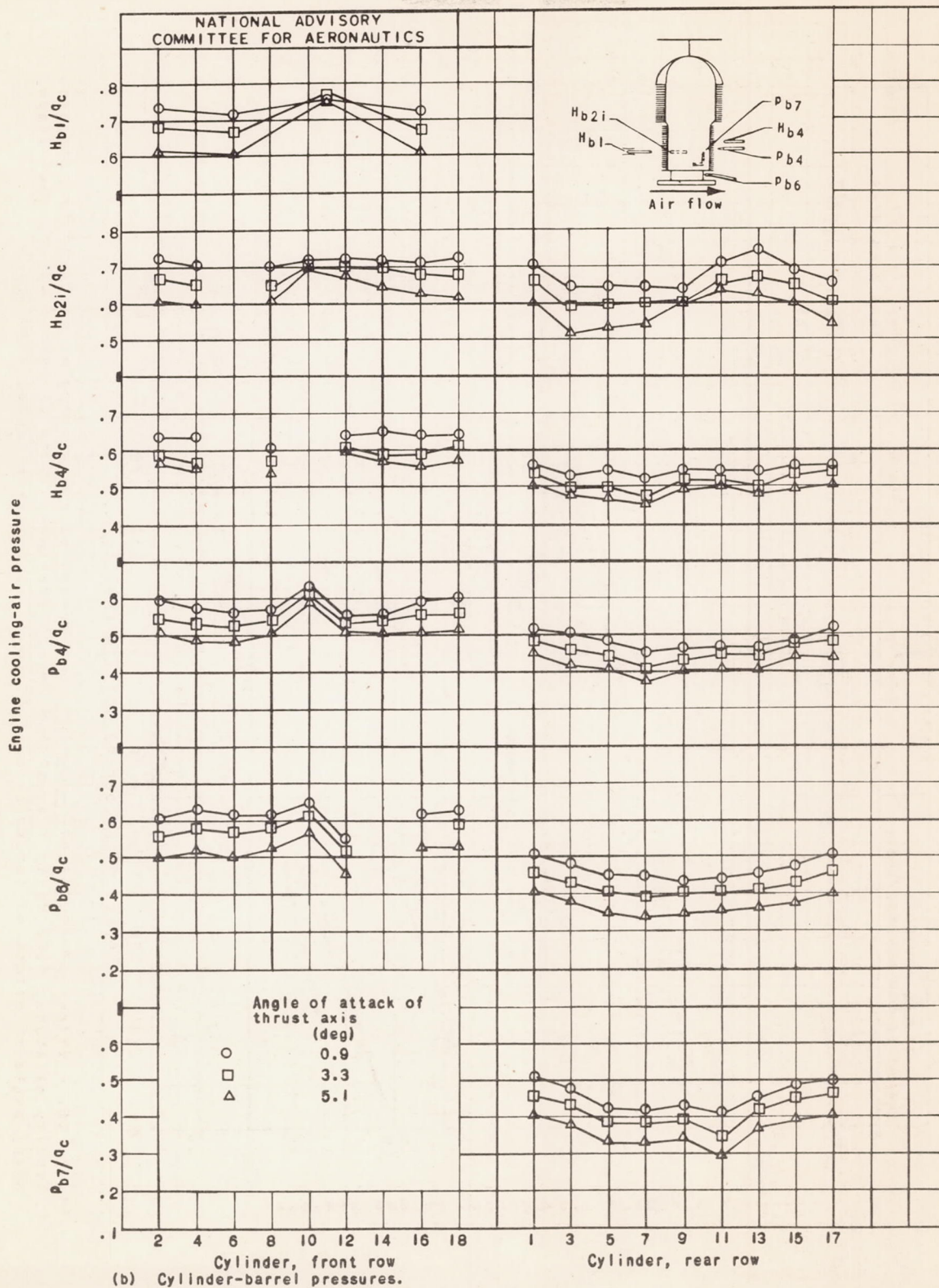


Figure 15. - Concluded. Effect of angle of attack of thrust axis on circumferential pressure distribution. Density altitude, 5000 feet; free-stream impact pressure, 19 to 22 inches water; cowl flaps, closed; thrust disk-loading coefficient, 0.09; propeller speed, 1200 rpm.



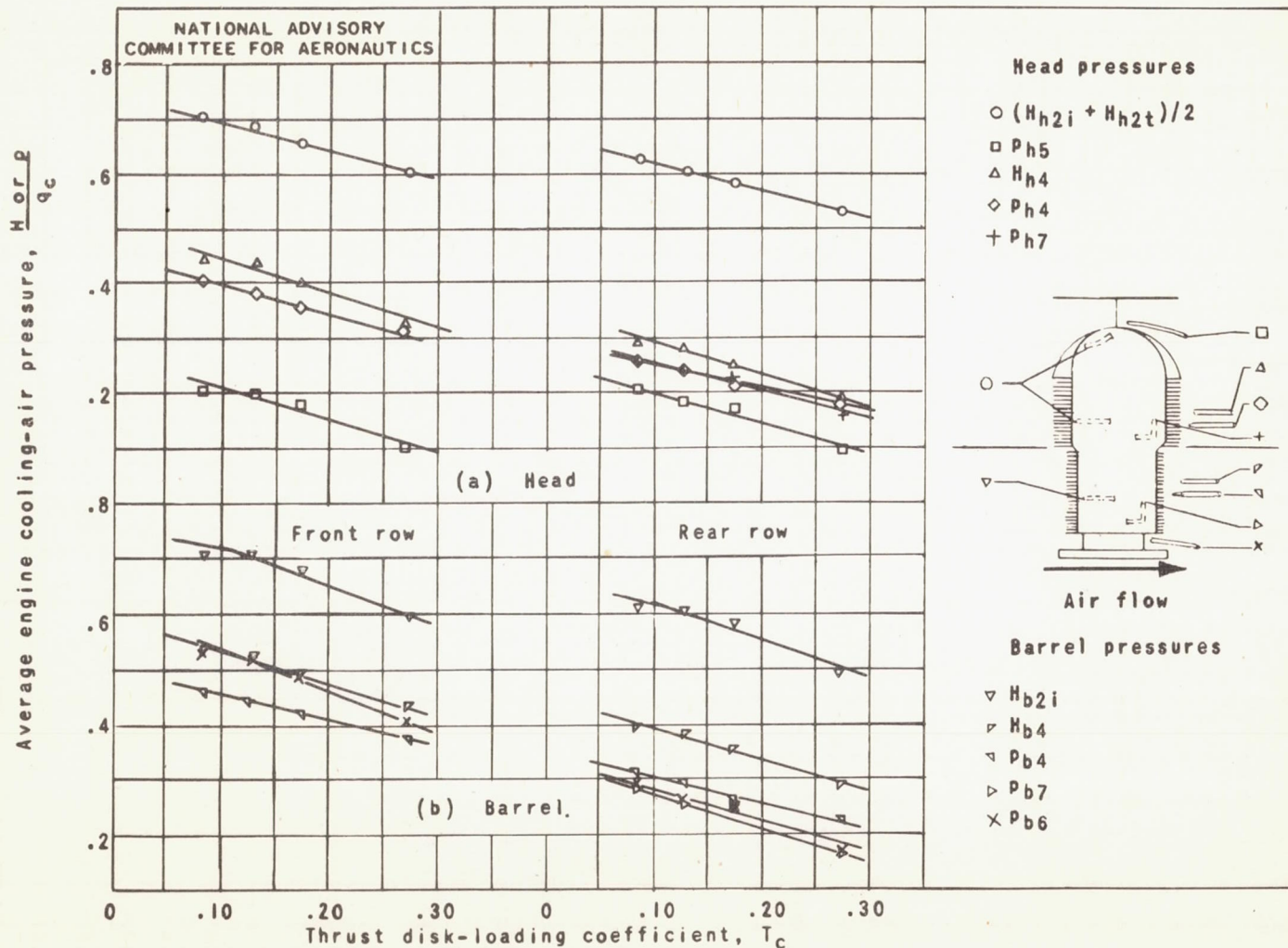


Figure 16. - Effect of thrust disk-loading coefficient on average engine cooling-air pressures. Density altitude, 5000 feet; free-stream impact pressure, 10 to 22 inches water; cowl flaps, open; angle of attack of thrust axis,  $1.8^\circ$  to  $3.7^\circ$ ; propeller speed, 1200 rpm.



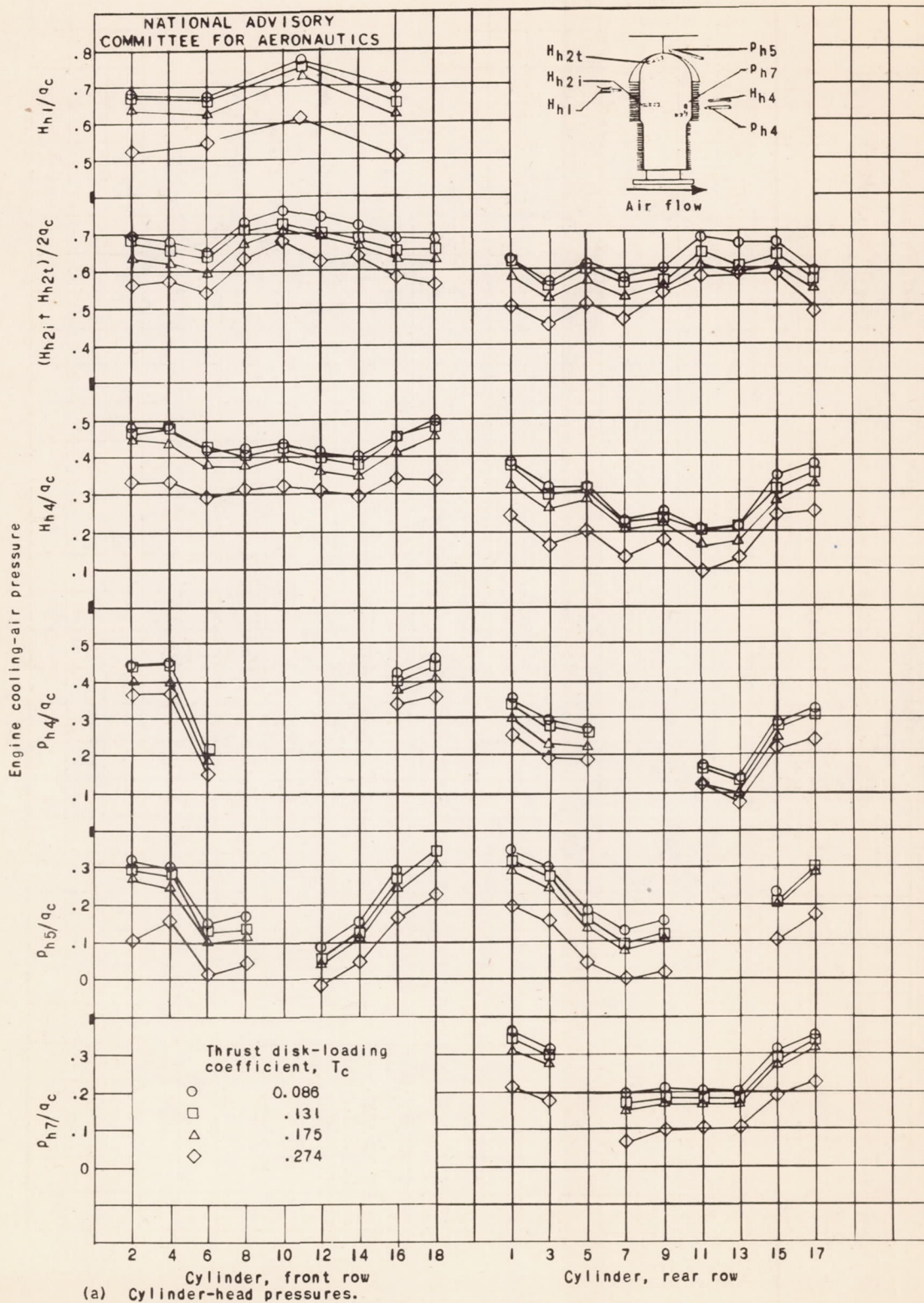


Figure 17. - Effect of thrust disk-loading coefficient on circumferential pressure distribution. Density altitude, 5000 feet; free-stream impact pressure, 10 to 22 inches water; cowl flaps, open; angle of attack of thrust axis,  $1.8^\circ$  to  $3.7^\circ$ ; propeller speed, 1200 rpm.

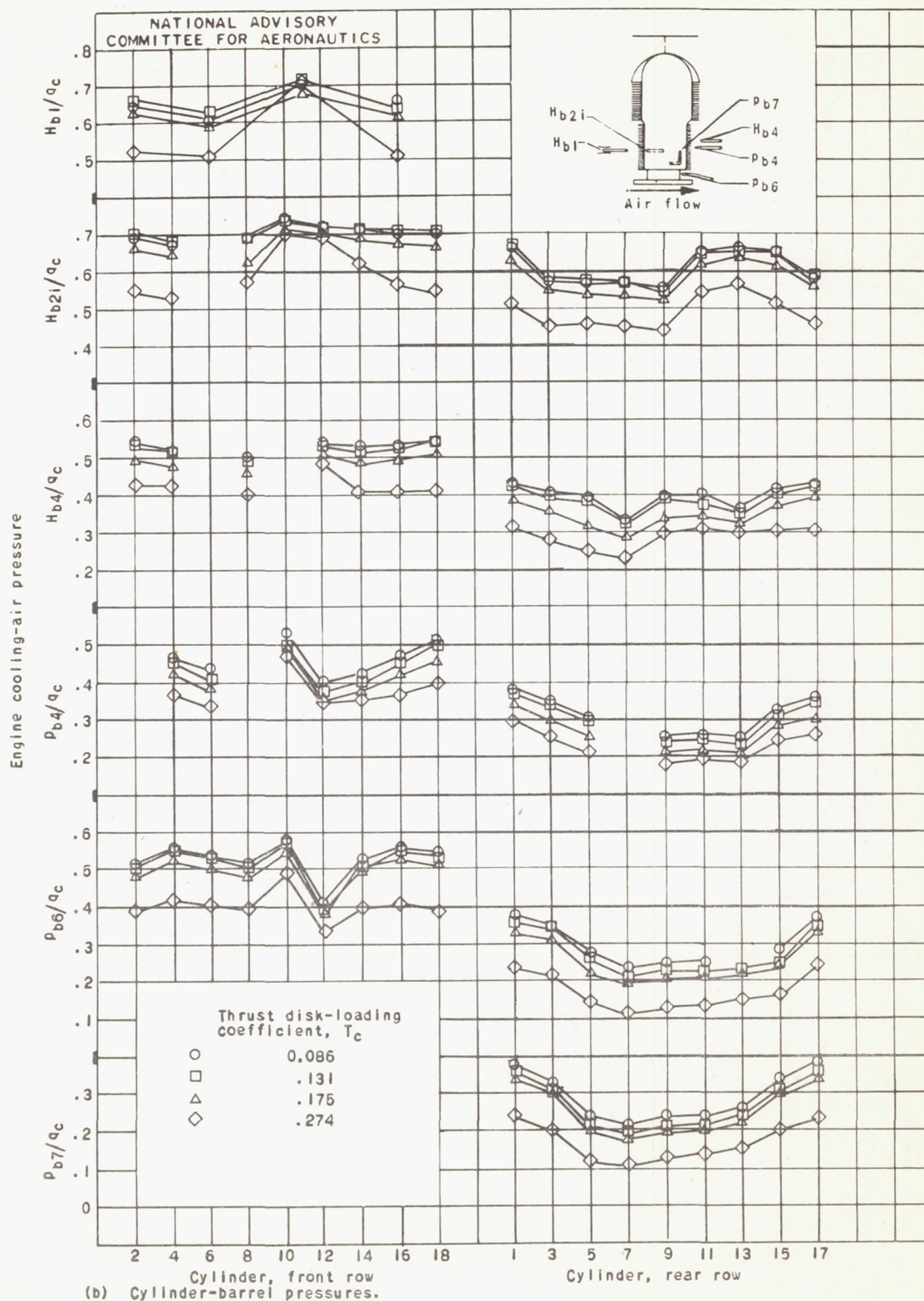


Figure 17. - Concluded. Effect of thrust disk-loading coefficient on circumferential pressure distribution. Density altitude, 5000 feet; free-stream impact pressure, 10 to 22 inches water; cowl flaps, open; angle of attack of thrust axis,  $1.8^\circ$  to  $3.7^\circ$ ; propeller speed, 1200 rpm.



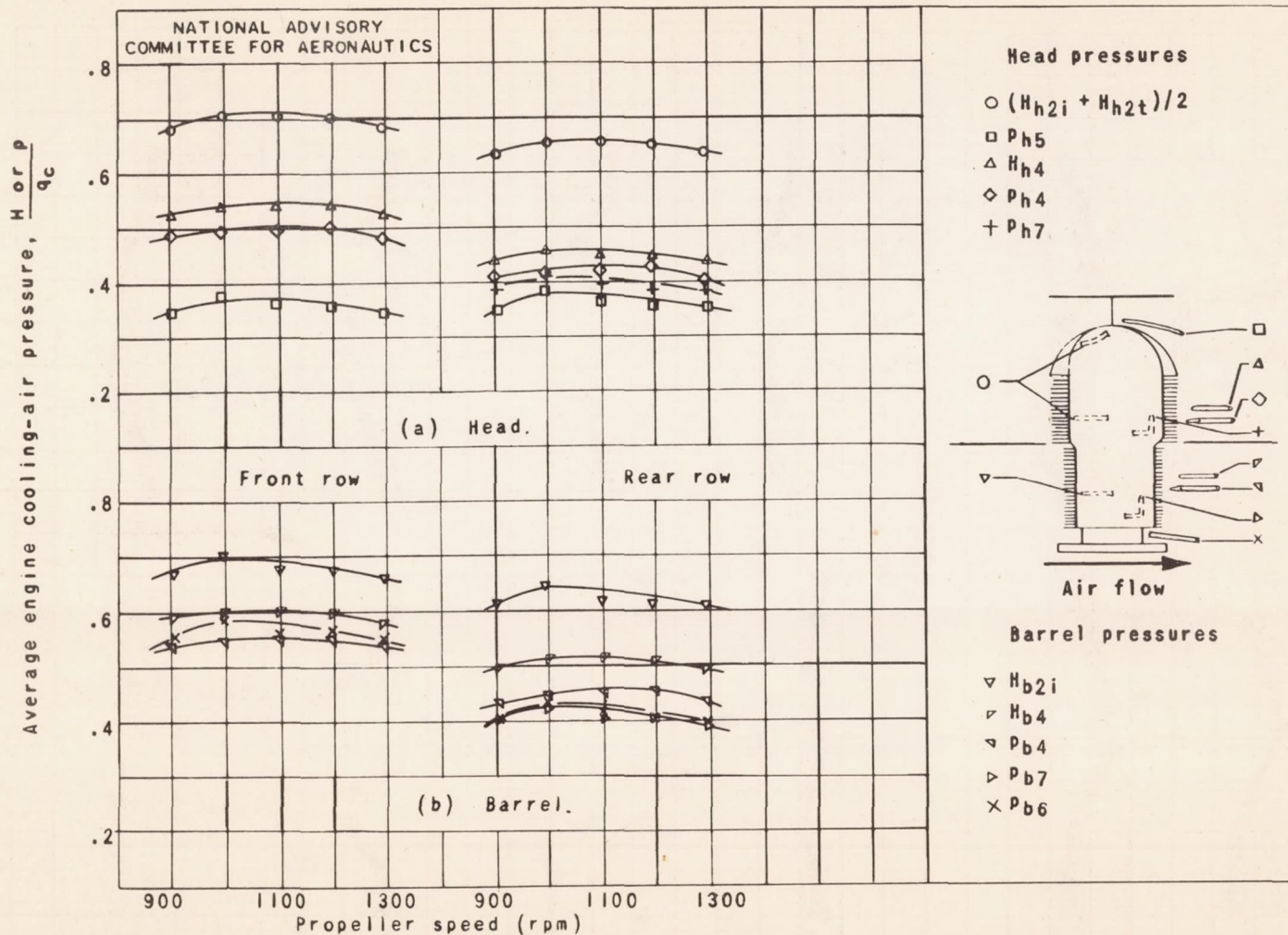


Figure 18. - Effect of propeller speed on average engine cooling-air pressures. Density altitude, 5000 feet; free-stream impact pressure, 21 to 22 inches water; cowl flaps, closed; angle of attack of thrust axis,  $3.1^{\circ}$  to  $3.4^{\circ}$ ; thrust disk-loading coefficient, 0.09.



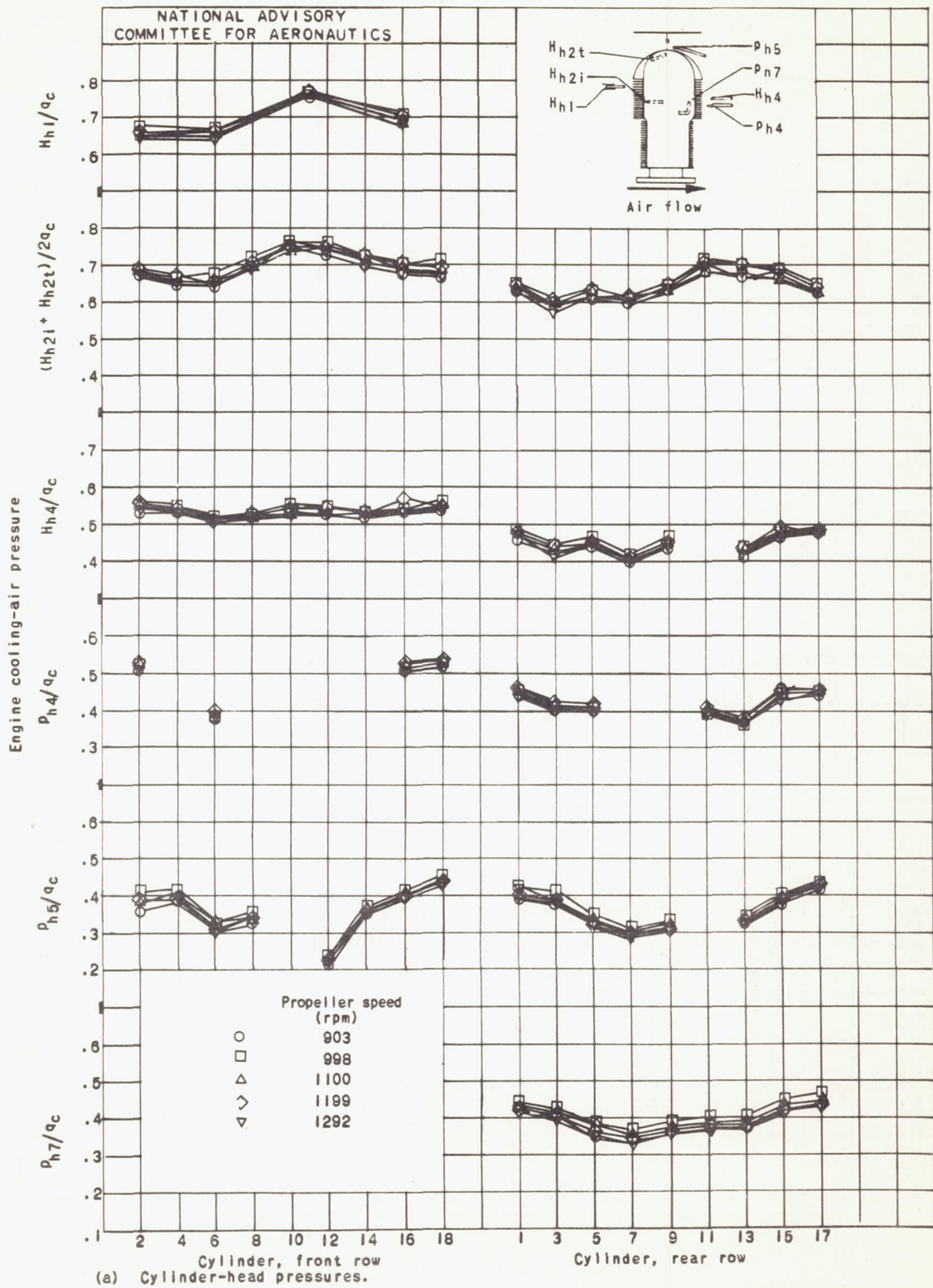


Figure 19. - Effect of propeller speed on circumferential pressure distribution. Density altitude, 5000 feet; free-stream impact pressure, 21 to 22 inches water; cowl flaps, closed; angle of attack of thrust axis,  $3.1^{\circ}$  to  $3.4^{\circ}$ ; thrust disk-loading coefficient, 0.09.

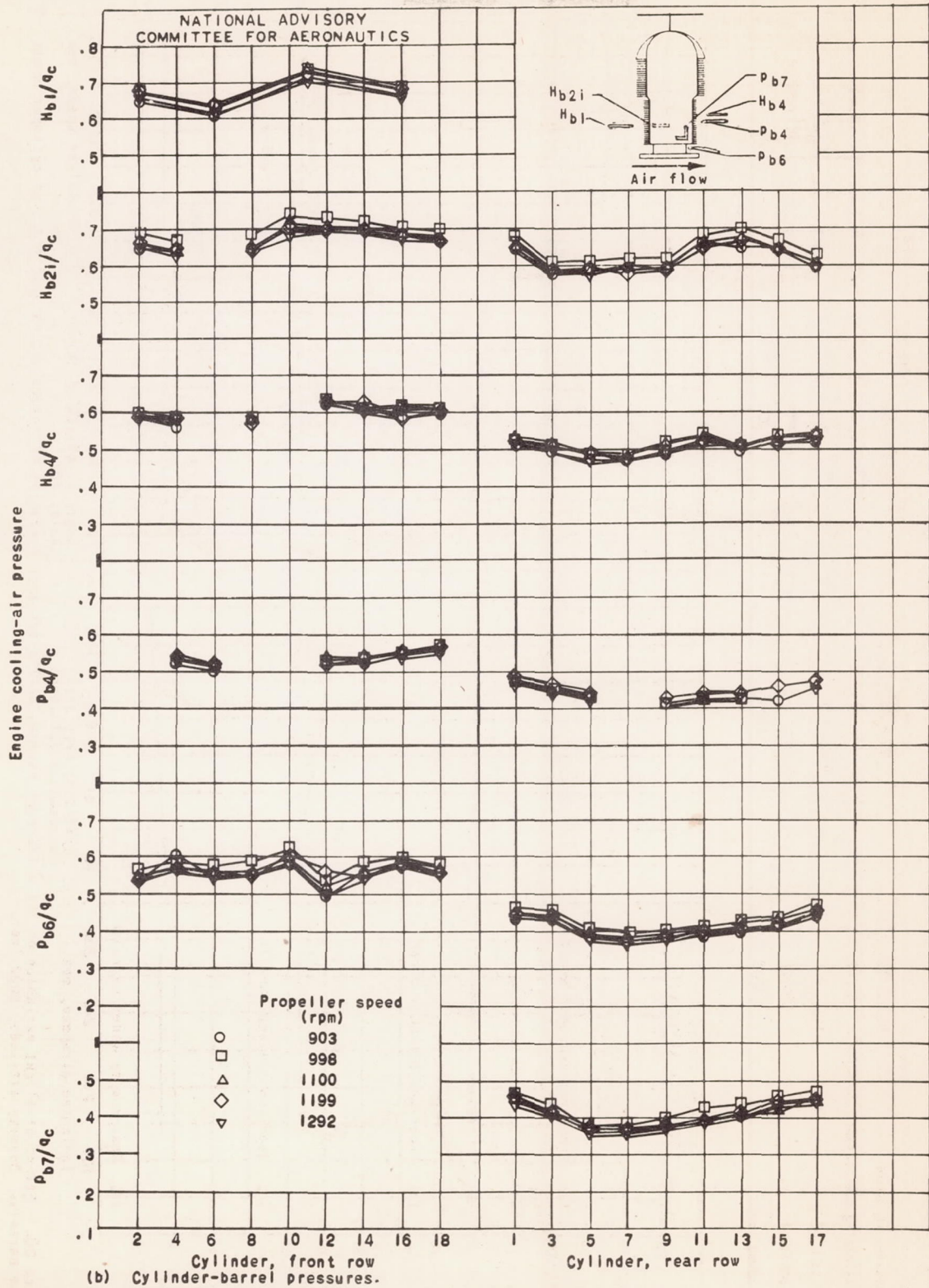


Figure 19. - Concluded. Effect of propeller speed on circumferential pressure distribution. Density altitude, 5000 feet; free-stream impact pressure, 21 to 22 inches water; cowl flaps, closed; angle of attack of thrust axis,  $3.1^{\circ}$  to  $3.4^{\circ}$ ; thrust disk-loading coefficient, 0.09.



Impact pressure, in. water	16.6 - 33	20 - 23	19 - 22	21 - 22
Thrust disk-loading coefficient	0.07 - 0.10	0.08 - 0.10	0.09	0.09
Angle of attack of thrust axis, deg	1.5 - 4.5	2.6 - 3.7	-----	3.1 - 3.4
Cowl-flap position	Closed	-----	Closed	Closed
Propeller speed, rpm	1200	1200	1200	-----

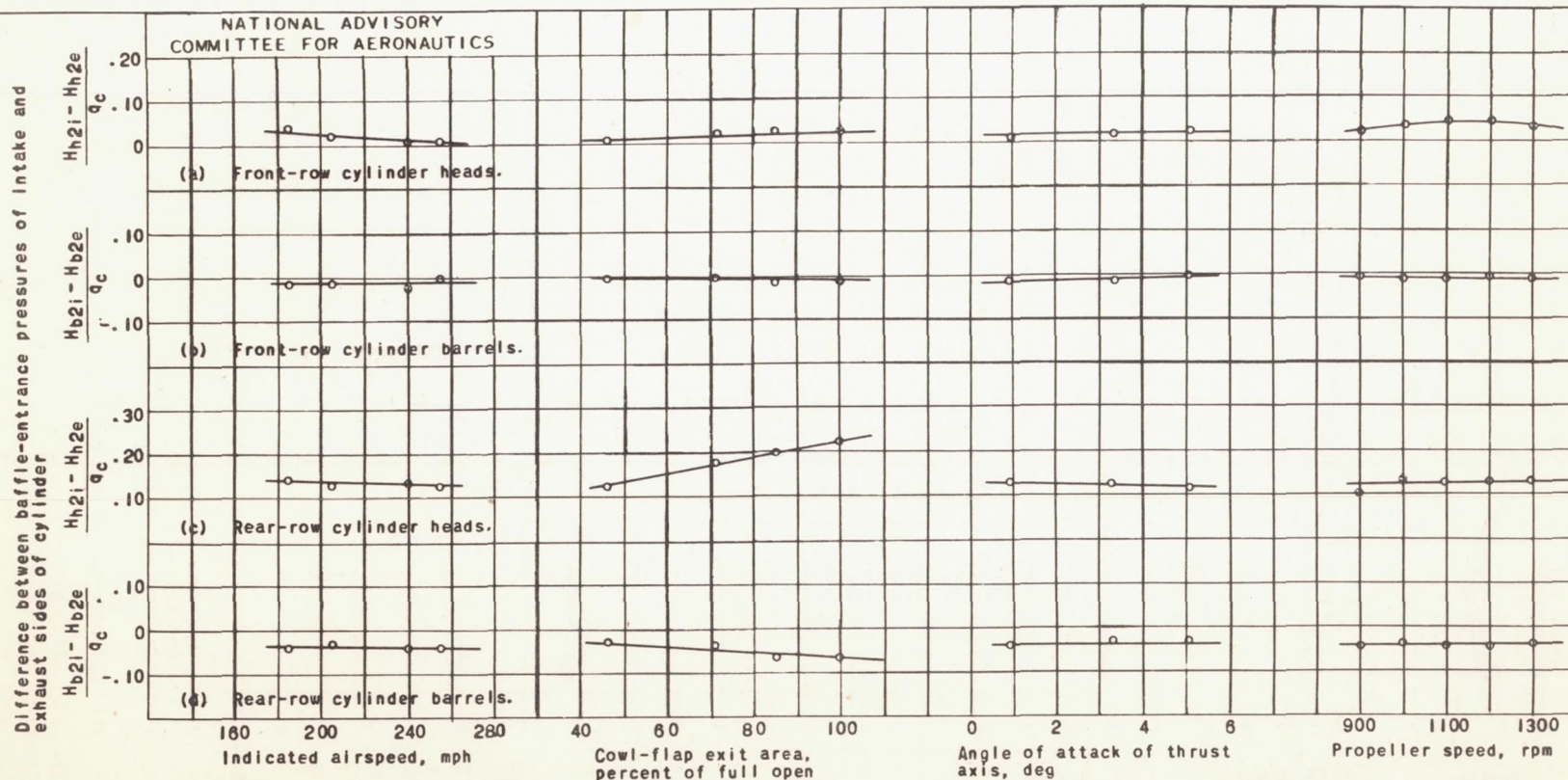


Figure 20. - Effect of flight variables on the difference between baffle-entrance pressures of intake and exhaust sides of cylinder heads and barrels. Density altitude, 5000 feet.



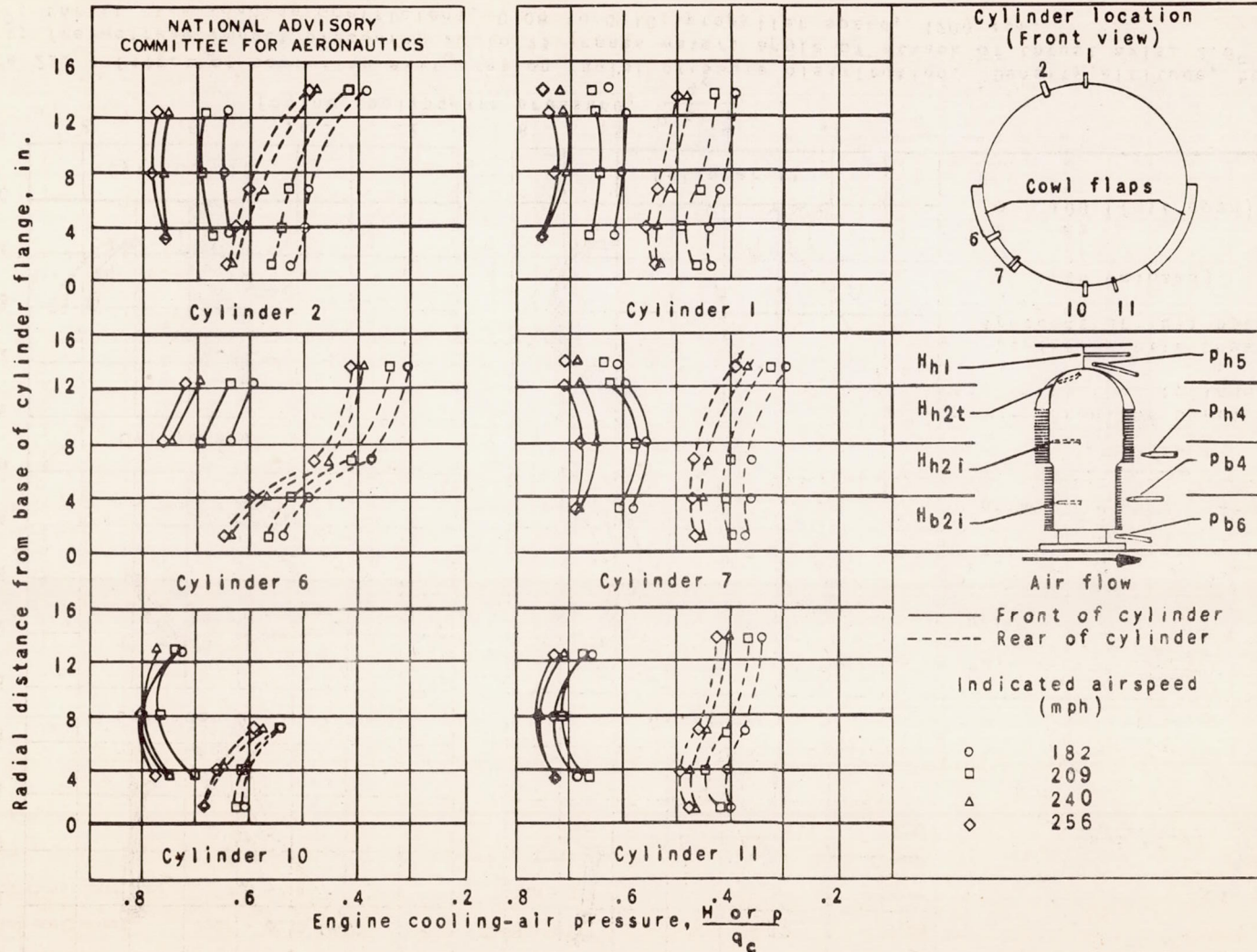


Figure 21. - Effect of airplane speed on radial pressure distribution during normal level flight. Density altitude, 5000 feet; cowl flaps, closed; propeller speed, 1200 rpm.

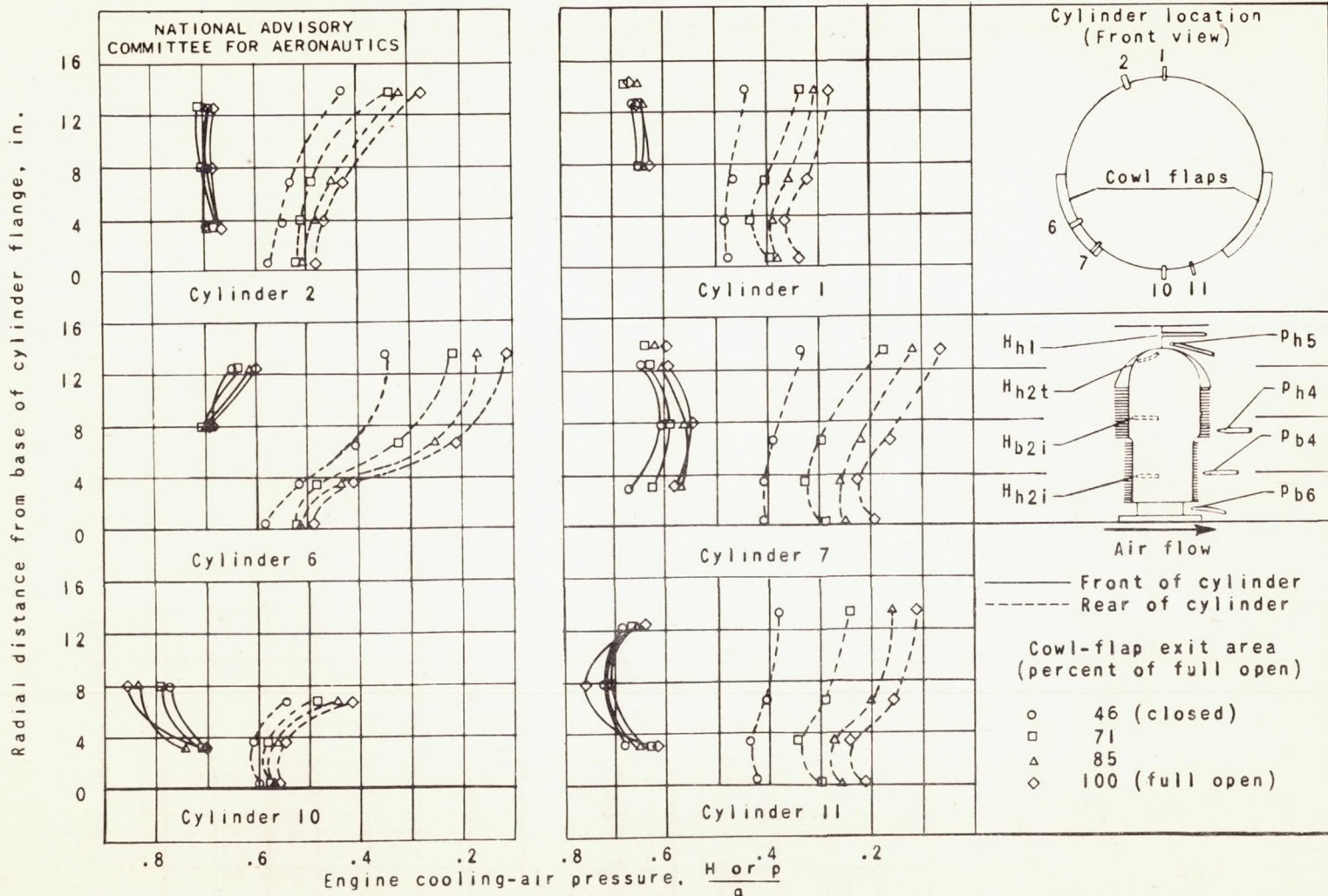


Figure 22. - Effect of cowl-flap exit area on radial pressure distribution. Density altitude, 5000 feet; free-stream impact pressure, 20 to 23 inches water; angle of attack of thrust axis,  $2.6^\circ$  to  $3.7^\circ$ ; thrust disk-loading coefficient, 0.08 to 0.10; propeller speed, 1200 rpm.



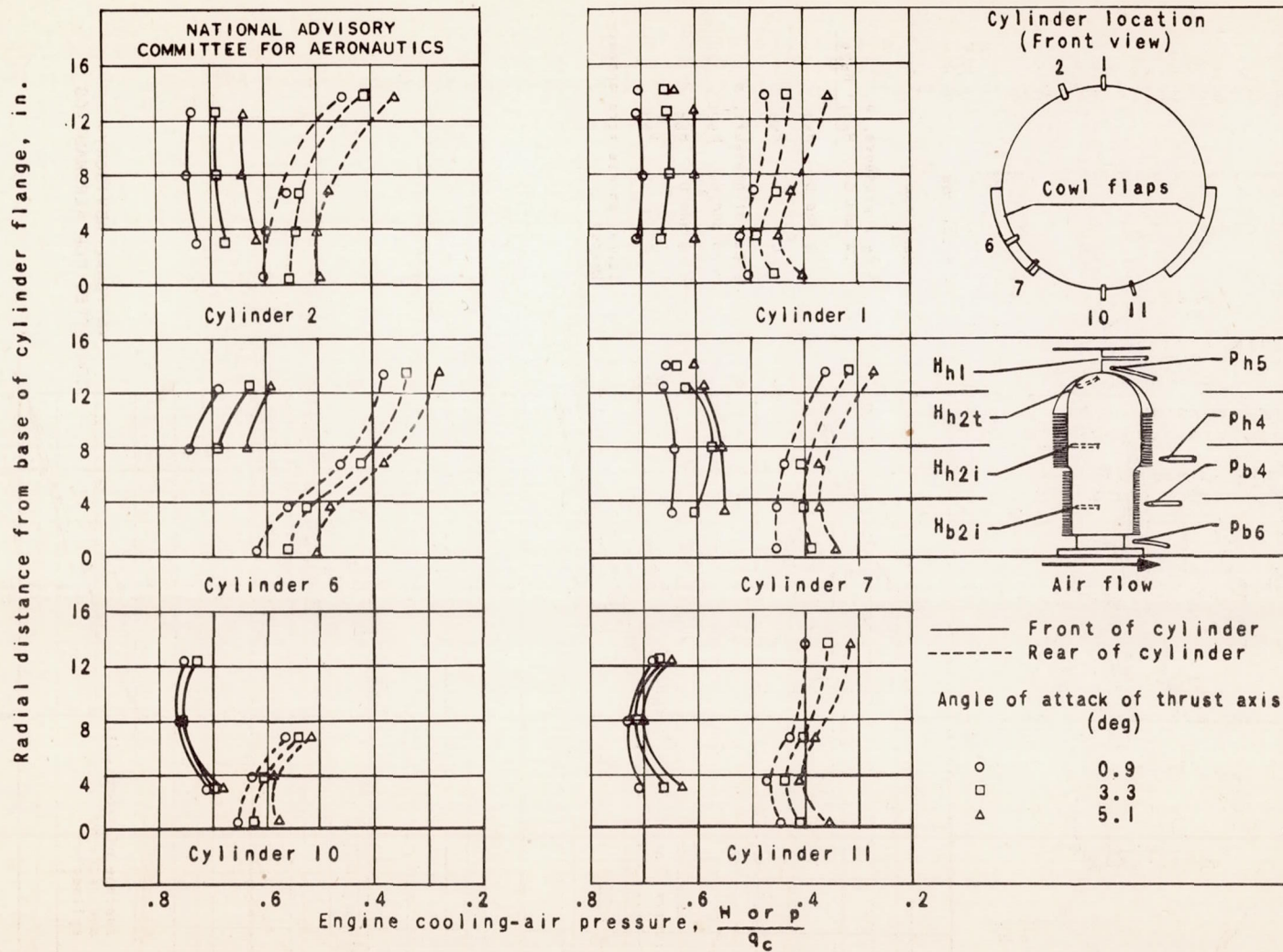


Figure 23. - Effect of angle of attack of thrust axis on radial pressure distribution. Density altitude, 5000 feet; free-stream impact pressure, 19 to 22 inches water; cowl flaps, closed; thrust disk-loading coefficient, 0.09; propeller speed, 1200 rpm.



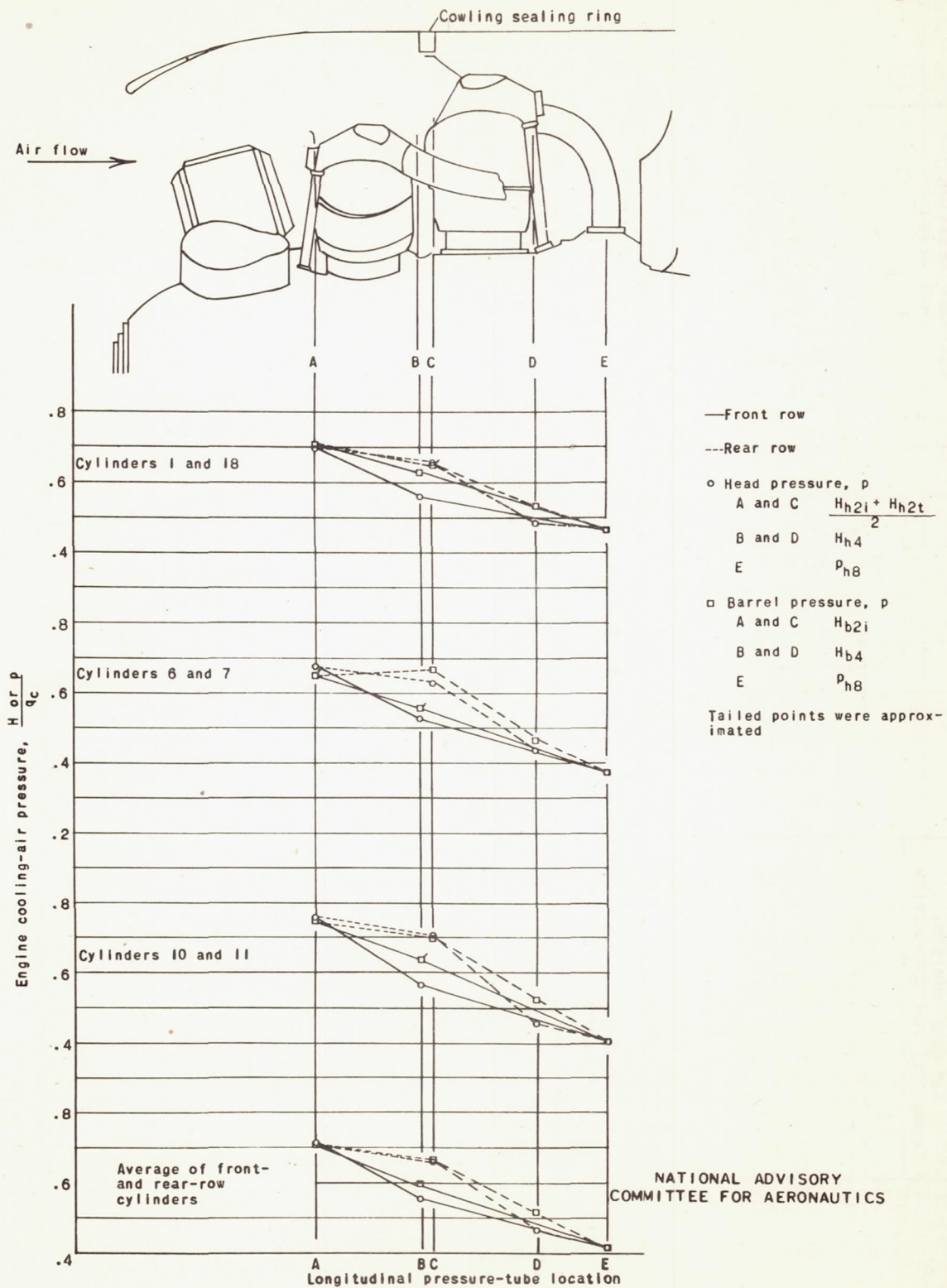


Figure 24. - Longitudinal pressure distribution for closed cowl flaps. Density altitude, 5000 feet; free-stream impact pressure, 23 inches water; angle of attack of thrust axis, 2.7°; thrust disk-loading coefficient, 0.08; propeller speed, 1200 rpm.

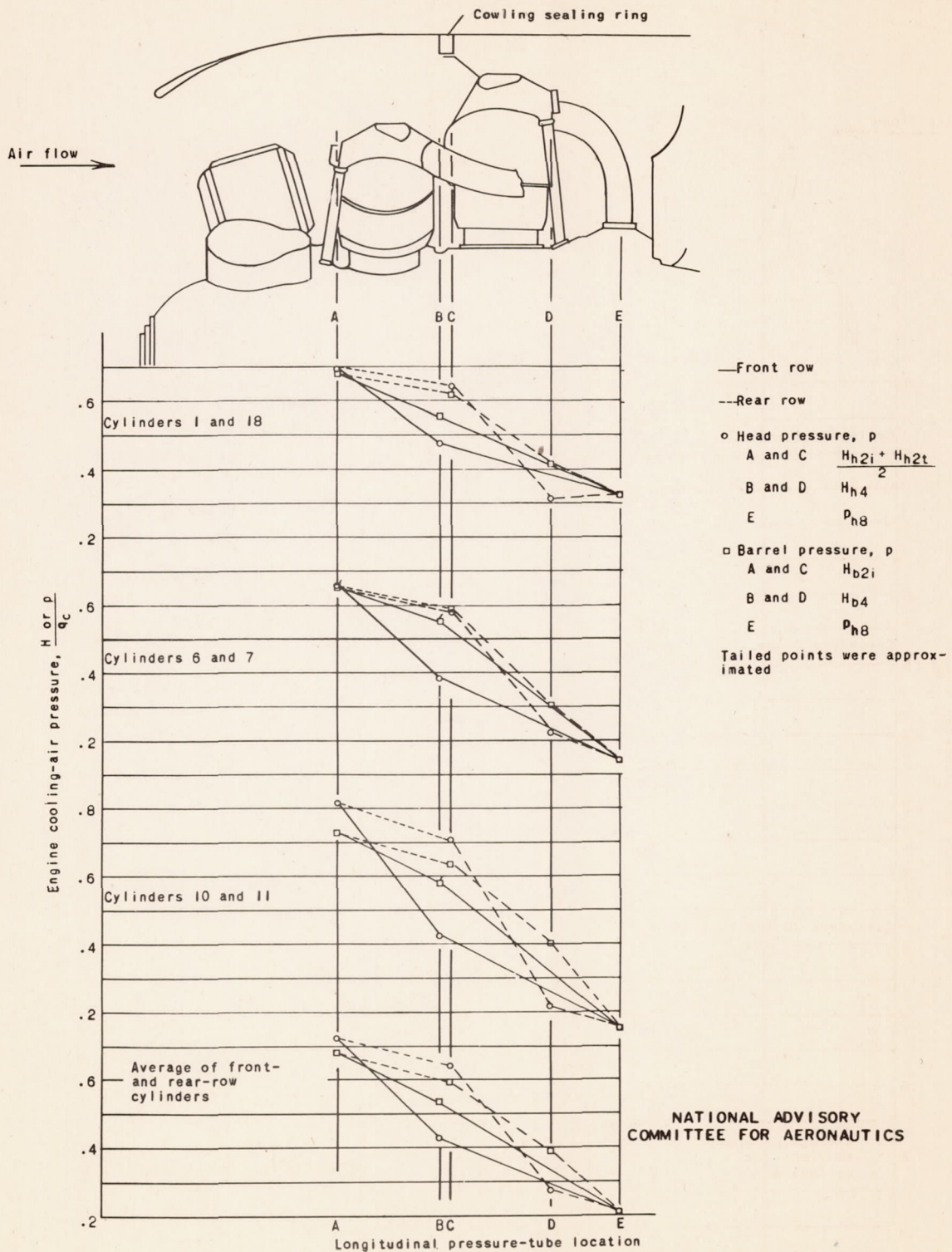


Figure 25. - Longitudinal pressure distribution for open cowl flaps. Density altitude, 5000 feet; free-stream impact pressure, 20 inches water; angle of attack of thrust axis,  $3.6^\circ$ ; thrust disk-loading coefficient, 0.10; propeller speed, 1200 rpm.